BER Report No. 149-02

AN INVESTIGATION OF THE UNSTEADY FLOW ASSOCIATED WITH PLUME INDUCED FLOW SEPARATION

by

Andrew L. Boggess, Jr.

Final Report on

Grant No. NGR-01-022-081

Prepared Under the Direction of

Julian O. Doughty, Ph.D.
Project Director

Submitted to

National Aeronautics and Space Administration
Langley Research Center
Hampton, Virginia 23365

Submitted by

Bureau of Engineering Research
The University of Alabama
University, Alabama 35486

July, 1972

BER Report No. 149-02

AN INVESTIGATION OF THE UNSTEADY FLOW ASSOCIATED WITH PLUME INDUCED FLOW SEPARATION

by

Andrew L. Boggess, Jr.

Final Report on

Grant No. NGR-01-022-081

Prepared Under the Direction of

Julian O. Doughty, Ph.D.
Project Director

Submitted to

National Aeronautics and Space Administration
Langley Research Center
Hampton, Virginia 23365

Submitted by

Bureau of Engineering Research
The University of Alabama
University, Alabama 35486

July, 1972

ABSTRACT

Rocket propelled vehicles which operate at high altitude produce large exhaust plumes which greatly modify the aerodynamic flow field. One of the most pronounced effects is an interaction between the plume bow shock and the vehicle boundary layer. The interaction results in a boundary layer separation which can produce several undesirable aerodynamic effects. A natural unsteadiness is inherent in the phenomenon (plume induced flow separation) and at present the only fluctuating pressure data available were taken on a Saturn V vehicle in flight. The data indicate fluctuating pressure levels of a magnitude to be of serious concern, particularly from a buffeting consideration. This report is a wind tunnel study of the basic nature of plume induced flow separation with emphasis on the unsteady aspects of the flow.

Testing was conducted in a 6 inch by 6 inch blow-down supersonic wind tunnel. A cone-cylinder model with a pluming jet was used as the test model. Test were conducted with a systematic variation in Mach number and plume pressure. Results of the tests are presented in the form of root-mean-squared surface pressure levels, power spectral densities, photographs of the flow field from which shock angles and separation lengths were taken, and time-averaged surface pressure profiles.

TABLE OF CONTENTS

LIST OF FIGURES

LIST OF SYMBOLS

d	diameter
f	frequency
G	dimensional power spectral density
h	step height
L	separation length
M	Mach number
P	free-stream mean-static pressure
Ps	mean static pressure at the separation point
P_1	mean static wall pressure
P_{rms}	root-mean-squared pressure of separated flow
P'_{rms}	root-mean-squared pressure of unseparated flow
Pp	plume stagnation pressure
q	free-stream dynamic pressure
R	Reynolds number
RMS	root-mean-squared
t	time
U	free-stream velocity
u	local velocity
X	direction along model
z	direction normal to the flow and parallel to the model surface
δ	boundary layer thickness
ϕ	deflection angle
θ	shock angle

CHAPTER I

INTRODUCTION

In the past few years, the unsteady effects of separated flows have become of increasing interest. This is due, in part, to the fact that flight vehicles are now operating in flow regimes with high dynamic pressures and are, therefore, subject to large pressure variations. The pressure fluctuations produced by attached turbulent boundary layers have been studied quite extensively, and the fluctuations are understood well enough that reliable estimates of their level can be made. However, it is also important to study the pressure fluctuations associated with separated flows since most vehicles have some portion of their boundary engulfed in separated flow.

Separated flows can be produced in a variety of ways, such as compression corners, shock waves intersecting a surface, deflection devices, jet plumes, etc. The jet plume induced separation is one of the most important and least studied separation phenomenon. Most high altitude rockets and missiles encounter this phenomenon, and it will exert a major influence on the aerodynamic characteristics of the space shuttle.

This study is a report of an experimental investigation of the basic nature of pressure fluctuations associated with

plume induced flow separation. In this section a discussion of the scope of the research is presented. Mechanics of the separation phenomenon are discussed in Section II along with a review of related experimental studies. A discussion of the test model, laboratory equipment, and testing procedure is included in Section III. In Section IV the experimental results are presented, and conclusions are drawn in Section V.

Purpose and Scope of Research

The primary purpose of this study was to obtain wind tunnel measurements of the pressure fluctuation in the vicinity of boundary layer separation on a vehicle with a pluming jet. The vehicle was scaled to a suitable size for mounting in a supersonic wind tunnel, and the plume was generated by a secondary air supply from a high pressure facility located near the wind tunnel.

Tests were conducted with a systematic variation of Mach number and plume stagnation pressure. Results of the investigation are presented in the form of root-mean-squared (RMS) surface pressure levels, power spectral densities of surface pressure, time-averaged pressure profiles in the vicinity of separation, and photographs of the flow field from which separation lengths and shock angles were taken.

CHAPTER II

DISCUSSION OF SEPARATED FLOW

This section is intended to provide a basic discussion of the separation phenomenon and its associated properties. Included in this section is a review of major studies concerning separated flows, especially those studies concerning unsteady separated flow.

The Mechanism of Flow Separation

In supersonic flow, a shock wave produces a sharp rise in pressure and will penetrate through the boundary layer to the sonic line when it impinges a solid boundary. Because of diffusion, the sharp pressure change across the shock will produce a strong but finite pressure gradient in the subsonic portion of the boundary layer. Depending on the magnitude of the gradient, the nature of the oncoming boundary layer, and the length of upstream diffusion, separation may occur. For example, in a compression corner with viscous flow the diffusion process will cause an adverse pressure gradient and may separate the boundary layer. Since separation reduces the initial pressure rise by decreasing the initial flow turn angle and since the mechanism of separation is dependent on this pressure rise, the inviscid external flow

and the viscous internal flow are interdependent due to a pressure interaction.

Bogdonoff and Kepler [3]* report measurements in connection with an oblique shock impinging on a flat wall carrying a turbulent boundary layer with $M \simeq 3$. Figure II-1 shows a sketch of their interpretation of the effect caused by a weak shock ($\phi = 7°$) and a strong shock ($\phi \geq 13°$). The weak shock reflection is very much like that expected on the basis of ideal-flow theory. When the strength of the shock is increased to 13° the reflected pattern contains a system of expansion and compression waves, and the boundary layer thickens greatly and tends toward separation. Separation was observed to occur at deflection angles greater than 9°. The pressure rise which leads to separation is independent of shock angle and has a value of $p_s/p \simeq 2$.

A typical shock induced separated flow is shown in Figure II-2, in which the principle flow regions are shown with a wall-pressure profile. The lower edge of the boundary layer, or the shear zone, breaks away from the wall very noticeably at the separation point. It is a linear feature with approximately a 13° incline to the surface. The upper boundary of the shear zone makes an angle of about 16.5° with respect to the wall, therefore, the region spreads with an angle of about 3.5°. Above the shear zone, the flow is virtually uniform supersonic flow. Below the shear

---

* Numbers in brackets refer to references in the List of References.

a. $\phi = 7°$

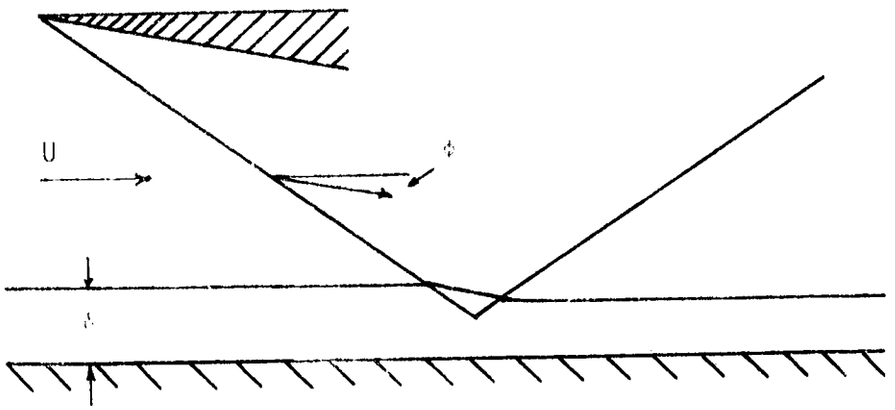

b. $\phi \geq 13°$

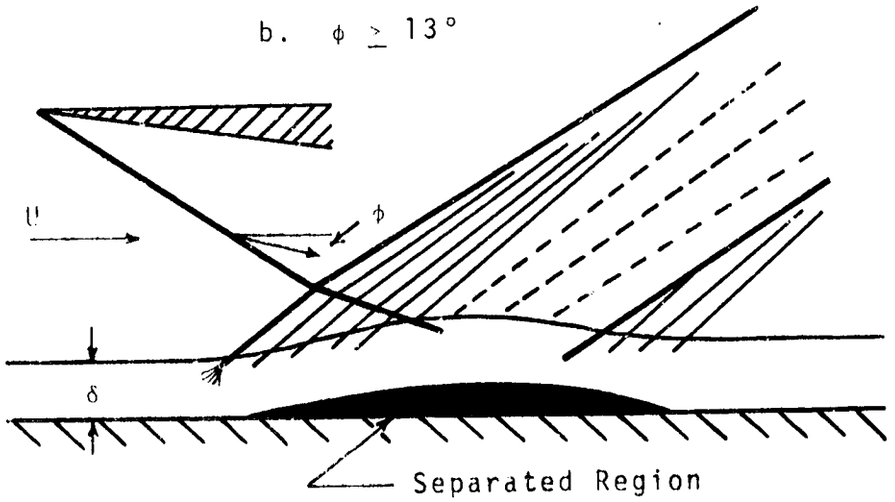

Figure II-1. Reflection of a Shock Wave from a Turburlent Boundary Layer on a Flat Wall, After Bogdonoff and Kepler [3]

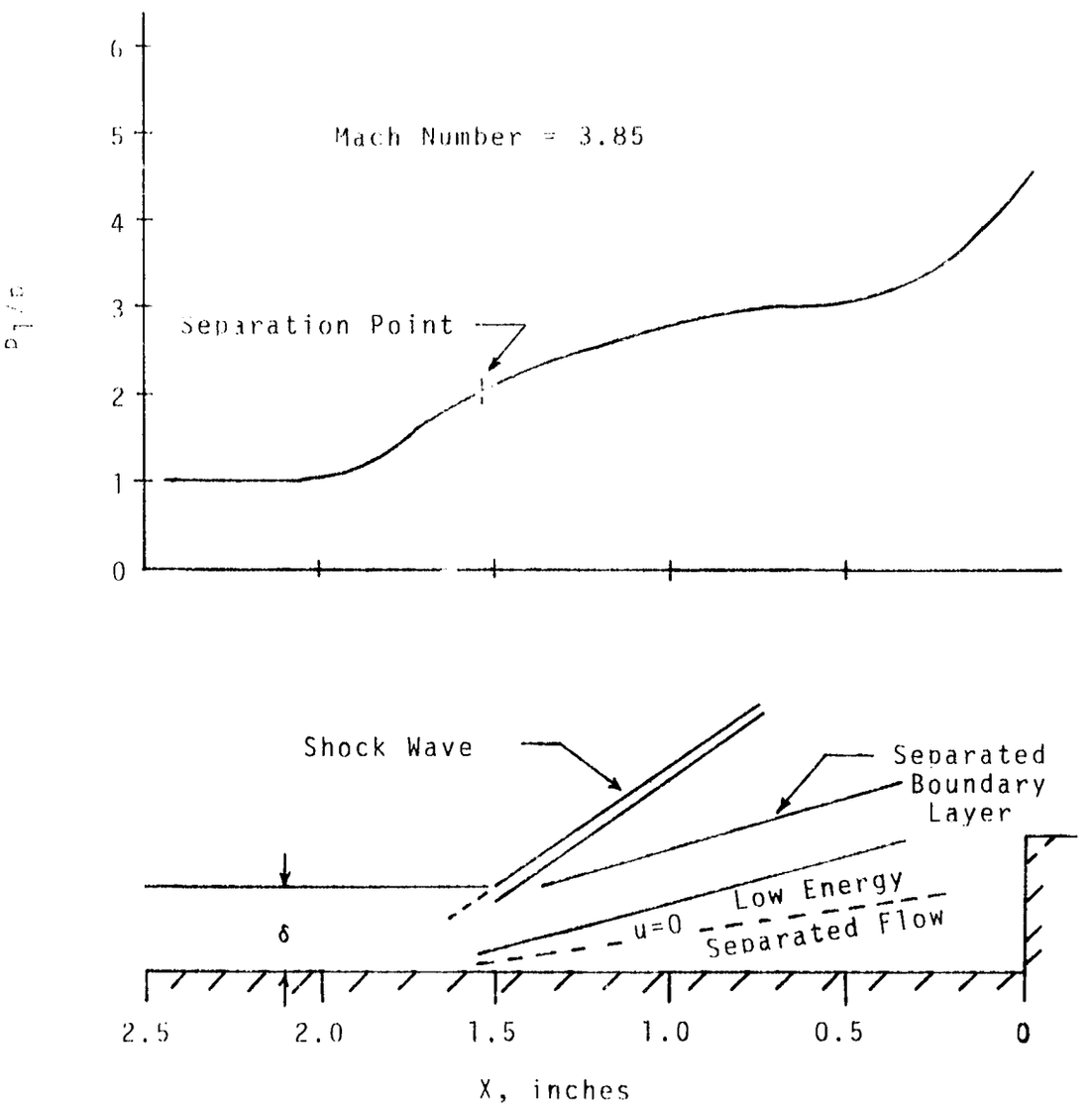

Figure II-2. Flowfield and Wall Pressure Distribution Produced by Separation of a Turbulent Boundary Layer Ahead of a Step, After Zukoski [20]

zone, the line along which u = 0 lies close to the center of a very strong recirculating region. The total pressure in this region is only 30% to 40% of the free-stream value, but the speed of the fluid is still as high as 35% of the free-stream value. [3,20]

Related Studies

A wide variety of research has been done in the separated flow regime in recent years. Bogdonoff and Kepler [3] studied separation due to a forward facing step, from which they obtained total and static pressure surveys of the separated region. Love [13] and Gadd [7] performed some of the first studies in which the Mach and Reynolds number influences were investigated. In 1958, Chapman, Kuehn and Larson [4] investigated separated flows with respect to the position of transition. Williams [19] and Mikesell [16] investigated the length of a separated region in a compression corner. Turbulent boundary layer separation induced by flares on cylinders was studied by Kuehn [12]. For compression corner flares, small separated regions (less than five boundary layer thicknesses) appeared to be as steady as the attached flow; however for larger separated regions the flow became unsteady, and the unsteadiness increased as the size of the separated region increased. When separation occured on the curved-surface flares, the flow was extremely unsteady. The unsteadiness was evidenced by the random shock pattern. Photographs taken in succession for

a given test condition showed the shock system to vary with time. It was also observed that the separation point oscillated over a distance of several boundary layer thicknesses.

Gillette [8] obtained static and total pressure surveys of turbulent boundary layer separation over a compression corner. In his investigation, it was found that separation exceeding six or eight boundary layer thicknesses became unsteady, in which the excursions of the separated point were less than half a boundary layer thickness. Zukoski [20] reports from some unpublished data by C. F. Coe of Ames Research Center, that near the separation point the ratio of pressure fluctuation (RMS values) to the free-stream dynamic pressure is roughly .06, and over the plateau region the ratio is about .03. These values are roughly independent of Mach number. Zukoski states that for Reynolds numbers two to three times the transition value, the overall features of separated flow become independent of Reynolds number. The pressure ratio for separation is almost constant with Mach number. Strike [18] studied the interaction between plumes and an external stream at a Mach number of 10. His test were conducted on a flat plate model with a three-dimensional plume exhausting at the trailing edge. These studies showed that in many respects the plume acts as a blunt body trailing the flat plate surface, which produces a large separated region on the model. However, unlike the blunt body, the plume is a moving fluid boundary which

appears to inject mass into the separated region and produces laminar boundary layer separation effects that differ from an equivalently shaped solid body. For instance, the pressure in the separated region was higher and more sensitive to the separation point than the same length of separated flow caused by a solid body. McGhee [14] investigated jet plume induced flow separation at Mach numbers of 3.00, 4.50, and 6.00 on various axisymmetric bodies. His primary result was that the separation angle and length were functions of jet pressure ratio and model geometry.

Of the many studies performed on the flow separation phenomenon, only a few people have investigated the unsteadiness associated with flow separation. Kistler [10,11] investigated the sidewall boundary layer on the Jet Propulsion Laboratory twenty inch supersonic wind tunnel. Separation was induced by a forward facing step on the order of one boundary layer thickness. The mean static pressure profiles obtained by Kistler were of the same general form of those obtained by Chapman [4]. The pressure rises rapidly near the separation point and then slowly approaches a peak. After this peak, the pressure dips slightly and then rises sharply near the step. Bogdonoff's [3] data differ only slightly from Kistler's, and this difference can probably be explained by three dimensional effects

Near the separation point, the qualitative features of the pressure fluctuations are quite different from those well within the separated region. (See Figure II-3)

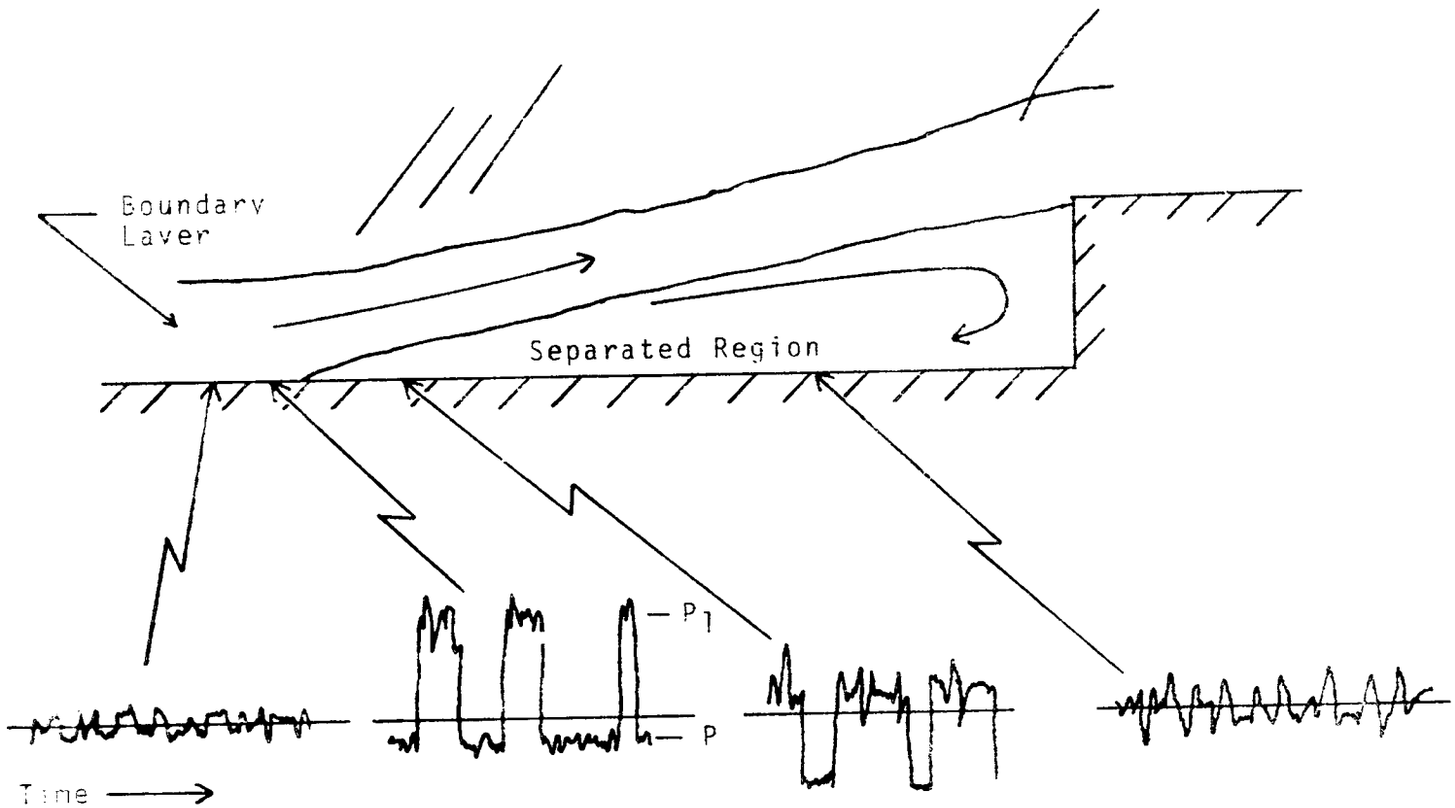

Figure II-3. Variation of the Wall Pressure with Time at Several Locations, After Kistler [11]

According to Kistler [10], the time history of a point well inside the separated region appears as a normal turbulence signal (a finite band of white noise). Near the separation point however, the signal has more of an "on-off" character and can best be described as a white noise superimposed on a random square wave of large amplitude. The frequency of the square wave is much less than 1 kcps. Pressure fluctuation data for a Mach number of 3.01 is shown in Figure II-4, where P_{rms} is the pressure level of the separation and P'_{rms} is the RMS pressure level of the unseparated region. Power spectral density data show that there is more energy at the low frequencies in the separated region than in the attached boundary layer. No spectra were obtained near the separation point since most of the energy was below 1 kcps, and the large fluctuations at the low frequencies made it difficult to obtain quantitative measurements. However, well within the separated region there is very little energy below 1 kcps.

Referring again to Figure II-3, the pressure jumps back and forth between P and P_1 at the separation point. The simplest explanation of this is that at any instance of time the wall pressure distribution is a step function, with the lower value P ahead of the separation point and the higher value P_1 in the separated region. The location of this jump is not stationary but moves over a restricted region. Kistler offers the following explanation for the motion of the separation point.

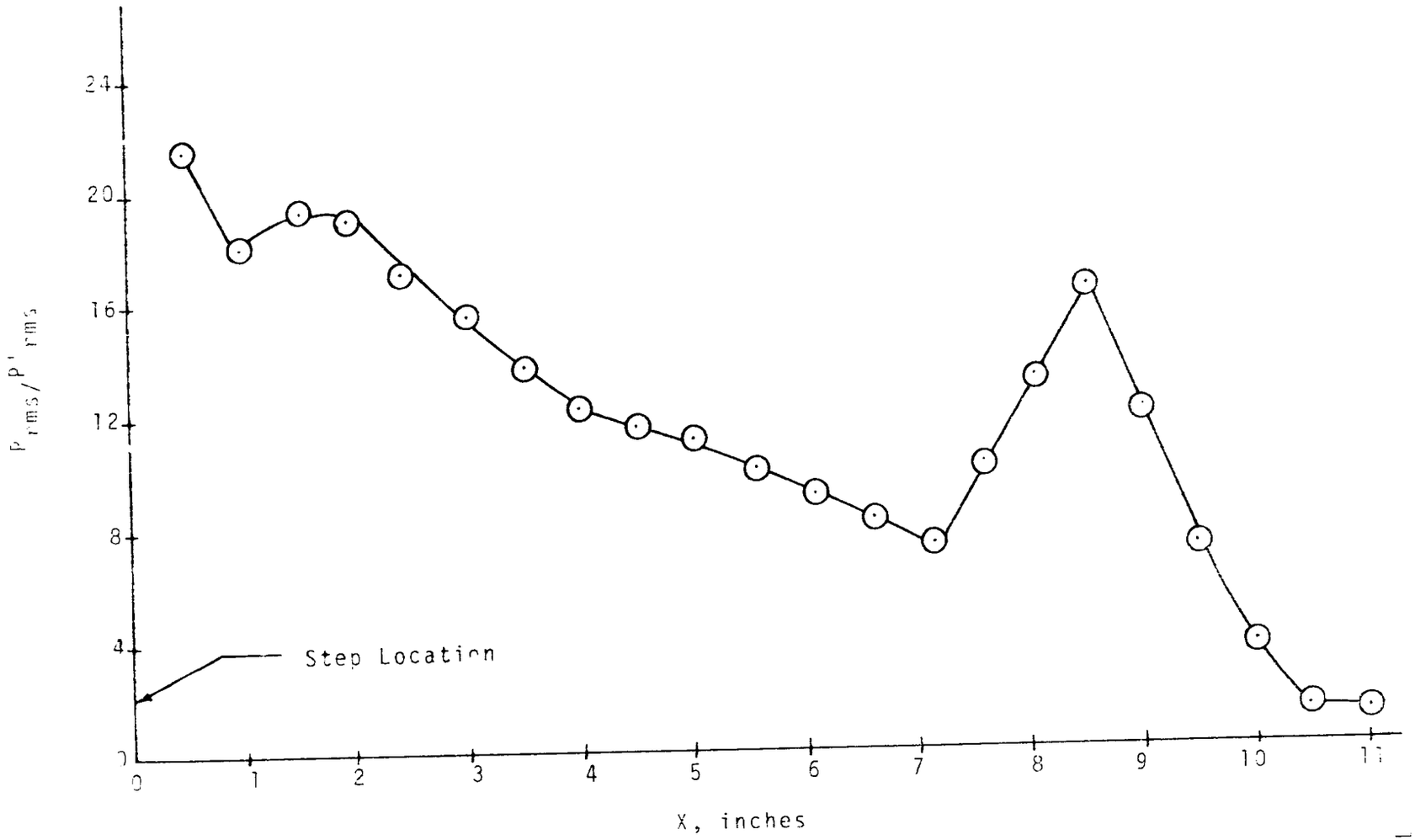

Figure II-4. RMS Pressure Fluctuation Level, After Kistler [11]

> The dividing surface is randomly distorted in the z direction. This conjecture is supported by the fact that the motion of the separation point is not observed in either still or motion pictures of the flow. The extent of this region (almost the entire region of the steep pressure rise) is big enough as compared to the boundary layer thickness that it certainly should be visible if the motion were uniform over the width of the separated region. A random variation in the z direction of the separated point, however, would be averaged in a picture normal to the flow. Futhermore, a cross-stream distortion of the flow is a plausible explanation of the observed effect since, for the supersonic flow, any perturbation that would increase the deflection angle of the dividing surface would increase the local pressure, push aside the slowly moving, low-density recirculating fluid, and increase the perturbation. Measurements by Kuehn have shown that a supersonic turbulent boundary layer can support a larger pressure rise without separating than that encountered for the step flow, so that some motion of the separation point is possible without contradicting his measurements. The motion of the separation point is limited because, if the angle gets too large, either a new separation bubble is formed ahead of the old one or some other mechanism intervenes. [11]

The fluctuating wall pressures inside the separated region appeared to be caused by the turbulence in the free shear layer. However, the power spectral density curves changed from point to point which implies that other mechanisms are also operating, but they are secondary in comparison to the free shear turbulence.

Recently an extensive investigation of pressure fluctuations associated with a separated turbulent boundary layer has been undertaken at NASA Ames Research Center by C. F. Coe [5]. Figure II-5 shows the pressure fluctuation data that were recorded for the flow in the vicinity of a detached shock wave ahead of a 45° wedge in supersonic flow.

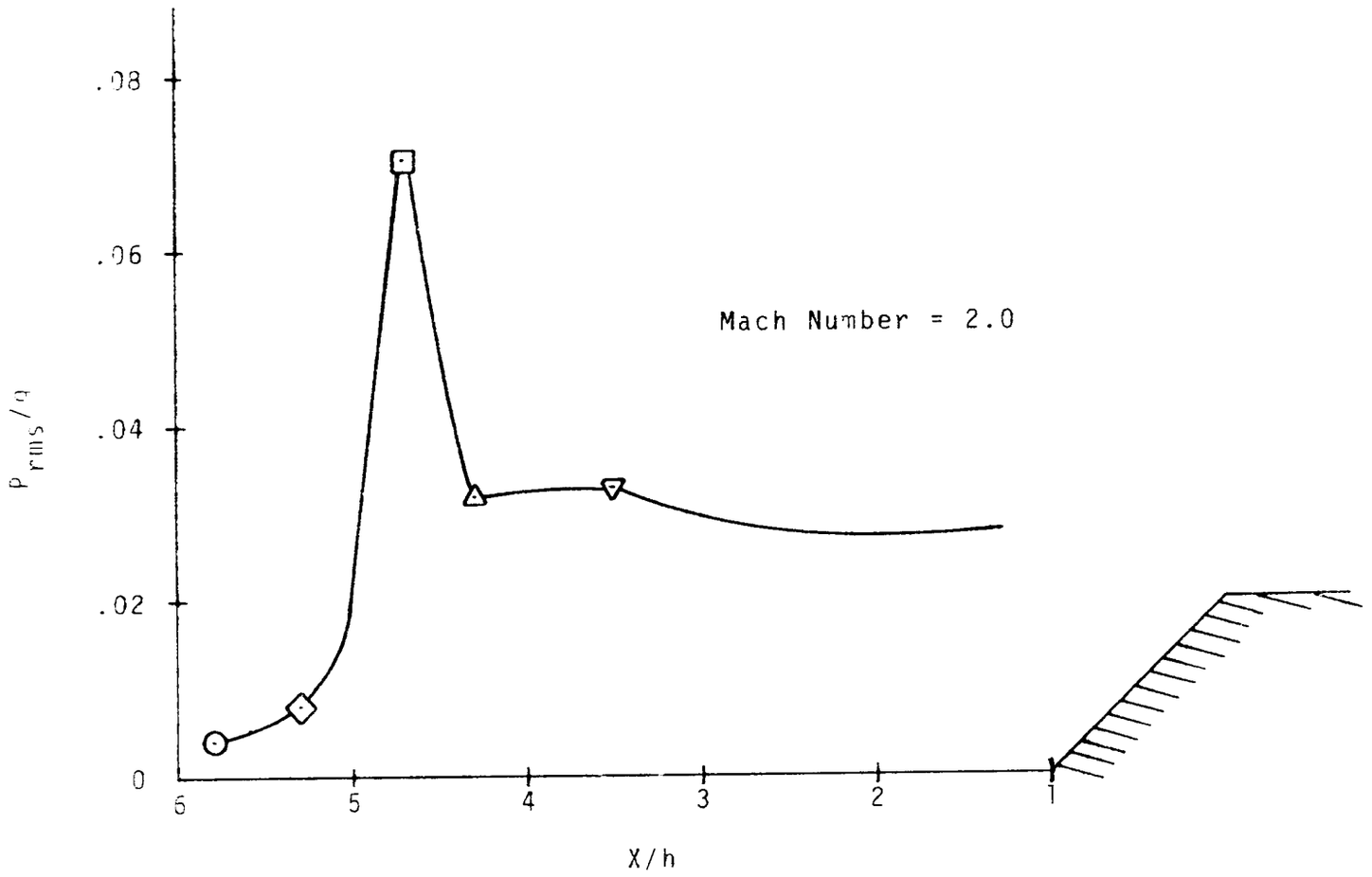

Figure II-5. Pressure Fluctuations in the Vicinity of Supersonic Flow Separation Ahead of a 45° Wedge, After Coe [5]

Coe observed three characteristic features of the broadband pressure fluctuation They are the low intensities of the attached boundary layer, the high intensity at the shock and a plateau level corresponding to the static pressure plateau region The power spectra, Figure II-6, show the distinct differences in each of the flow regions.

The only fluctuation data available on plume induced flow separation came from inflight measurements made on the Saturn V vehicle reported by Jones [9]. Photographic data were taken by a chase plane during the second flight of the Saturn V, AS-502. and it was noted that separation began about 90 seconds into the flight. As the vehicle gained altitude, the exhaust plume caused enlargements in the separated region and, consequently, there was a very rapid and violent forward movement of the separation front on the vehicle. Figure II-7 shows the movement of the separation front as taken from the film. At 150 seconds, near booster shut-off, the separated region completely engulfed the S-IC stage. If a similar separated flow occurs on the space shuttle, approximately 60% of the vehicle will be immersed in the separated flow region

Ten dynamic pressure transducers were mounted on the AS-505 vehicle in an effort to obtain pressure fluctuation data near the separation point The pressure histories of two of these transducers are shown in Figure II-8. The fluctuating pressure levels were unexpectedly high, and as

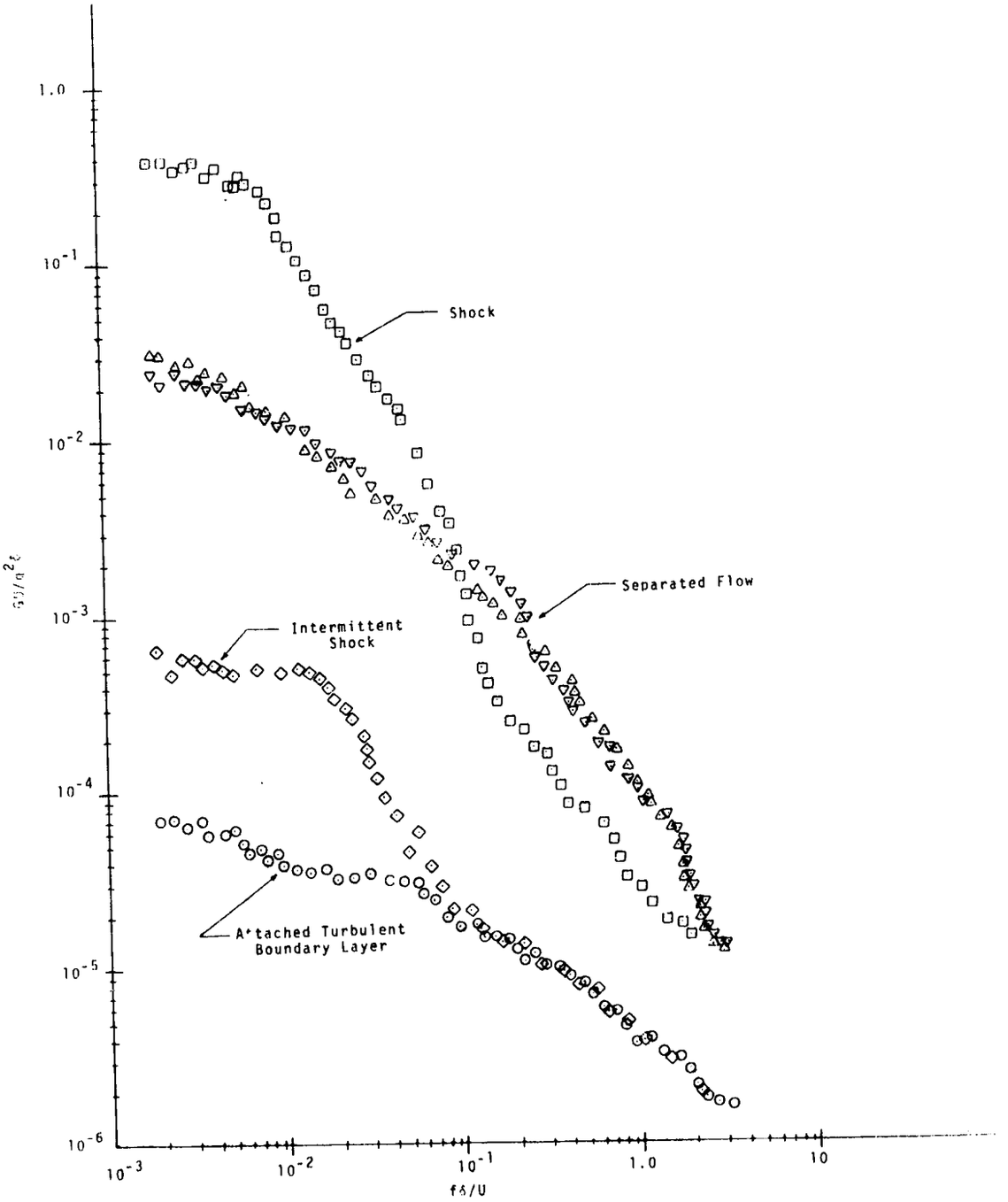

Figure II-6. Power Spectral Densities in Vicinity of Supersonic Flow Separation Ahead of a 45° Wedge, After Coe [5]

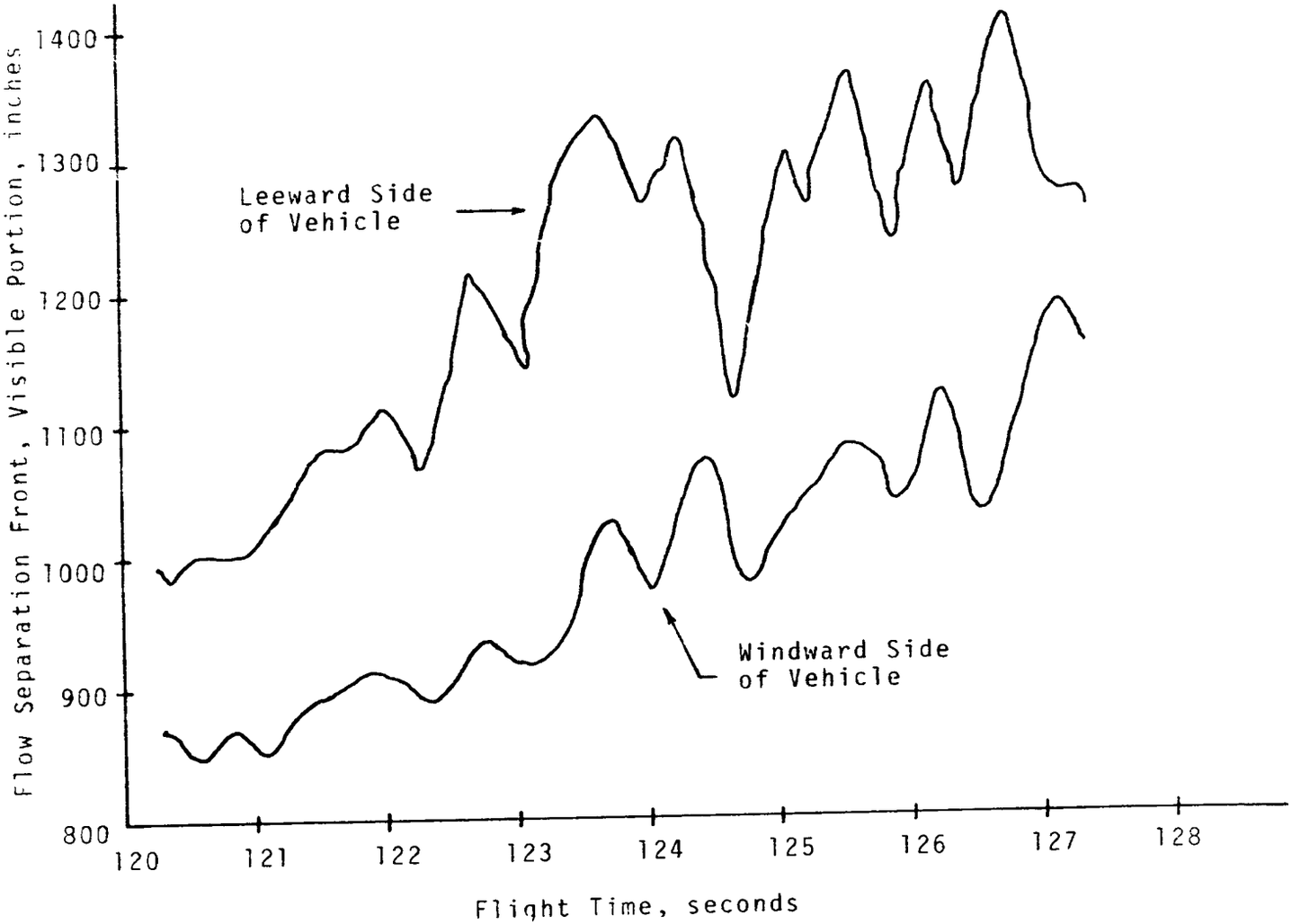

Figure II-7. AS-502 Flow Separation Front Versus Flight Time, After Jones [9]

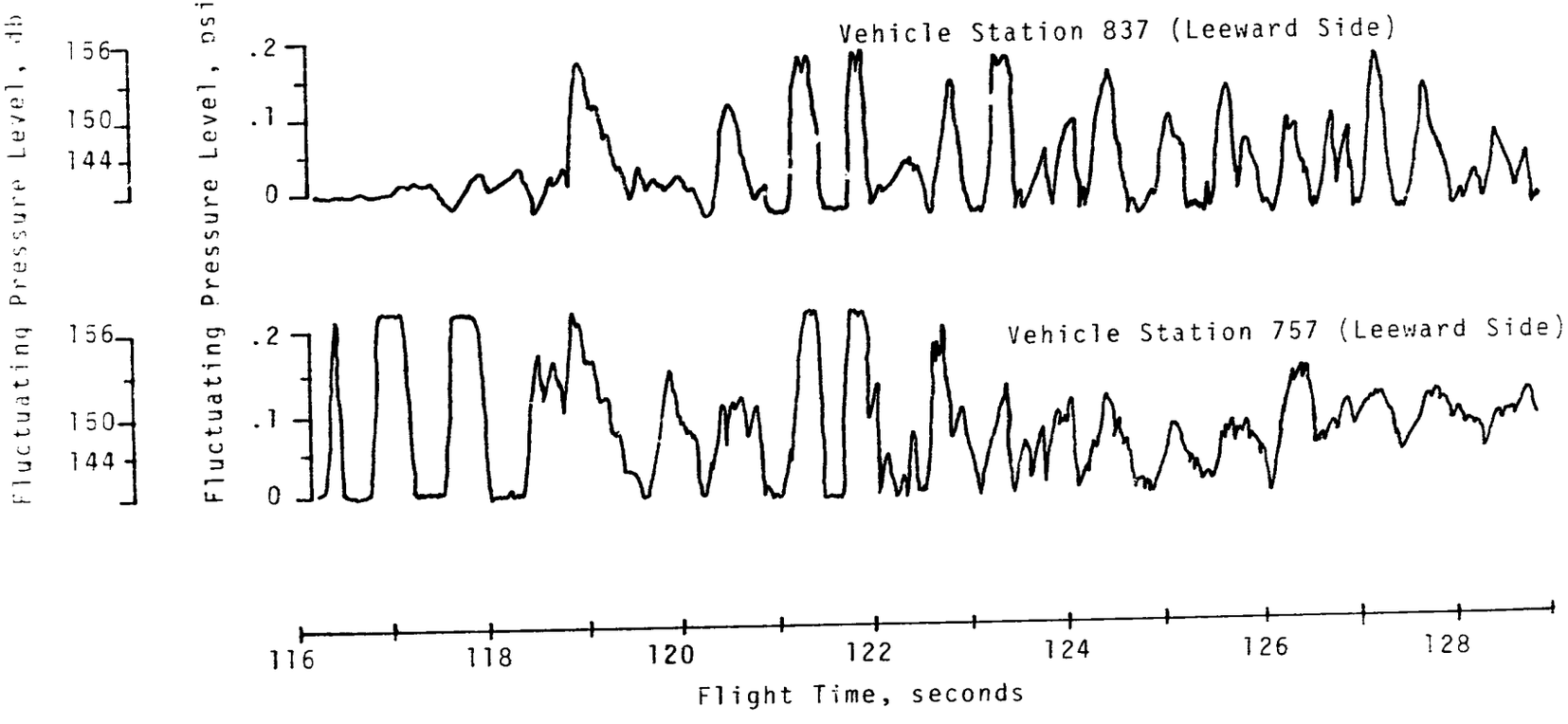

Figure II-8. Fluctuating Pressure in Region of Plume Induced Flow Separation, AS-505, After Jones [9]

a result, the signals were initially clipped as the separation front passed over the transducer. The pressure levels gradually decayed as the front continued forward. The clipping of the fluctuating signal was due to the fact that the instrumentation system was biased for a maximum of about 158 db. As can be seen in Figure II-8, the clipped signals could have exceeded 158 db by a considerable amount. It is also important to note that the pressure fluctuations showed a dominant frequency of 2 to 3 hertz.

CHAPTER III

EXPERIMENTAL APPARATUS AND PROCEDURE

The tests described in this report were conducted at The University of Alabama in Tuscaloosa during the time period from May 1971 to May 1972

Facilities used were those belonging to The University of Alabama and electronic and recording equipment kindly loaned by Marshall Space Flight Center.

Model Description

The model used in this study was designed to mount on the wind tunnel wall, in order that pressure taps, pressure transducers, and the high pressure line for producing the plume could be fabricated into the model with no interference generated in the primary flow. The brass model was mounted with the axis of symmetry located at the tunnel boundary layer displacement thickness. This reduced the boundary layer effect to a minimum, and also allowed a larger diameter body to be used than would have been possible on a sting mount. The overall configuration and dimensions of the model are shown in Figure III-1. A .250 inch wide lightly knurled band was machined around the body of the model just aft of the cone-cylinder intersection to

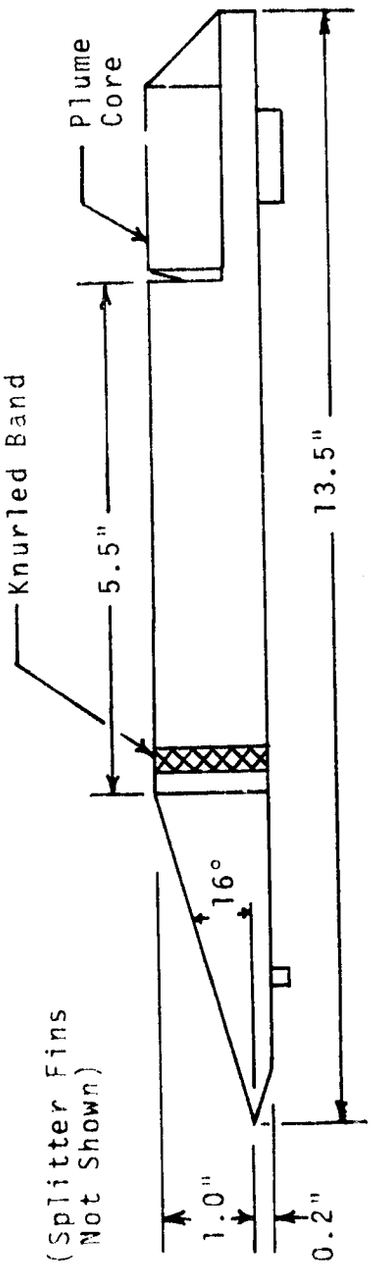

Figure III-1. Overall Configuration of the Test Model

trip and insure a turbulent boundary layer. It was necessary to machine a flat surface along the top of the model in order that the pressure transducers could be mounted flush with the model surface. The strip was 1/4 inch wide and approximately .007 inch of the diameter was removed. The nose cone angle and length of body were optimized in order that the leading shock cone would not reflect off of the tunnel walls and interfere with the flow pattern.

Stainless steel splitter fins were positioned on the model as shown in Figure III-2. The fins served to separate the tunnel boundary layer from the plume and were 1/16 inch thick with a 10° half wedge cut on the lower surface leading edge. This produced flat plate fins as seen by the flow on the upper surface. The leading edge of the fins were swept 70° so that the distance from the leading edge to the separated region was a minimum, thus minimizing the effect of the fin boundary layer.

The plume producing portion of the model is detailed in Figure III-3. In order to restrict the flowrate requirements a solid plume core was inserted. The core also provided a settling chamber for the plume. Both walls of the nozzle were conical, with the apex of the cones on the axis of the model. The nozzle was designed to produce an isentropic exit Mach number of 2.94

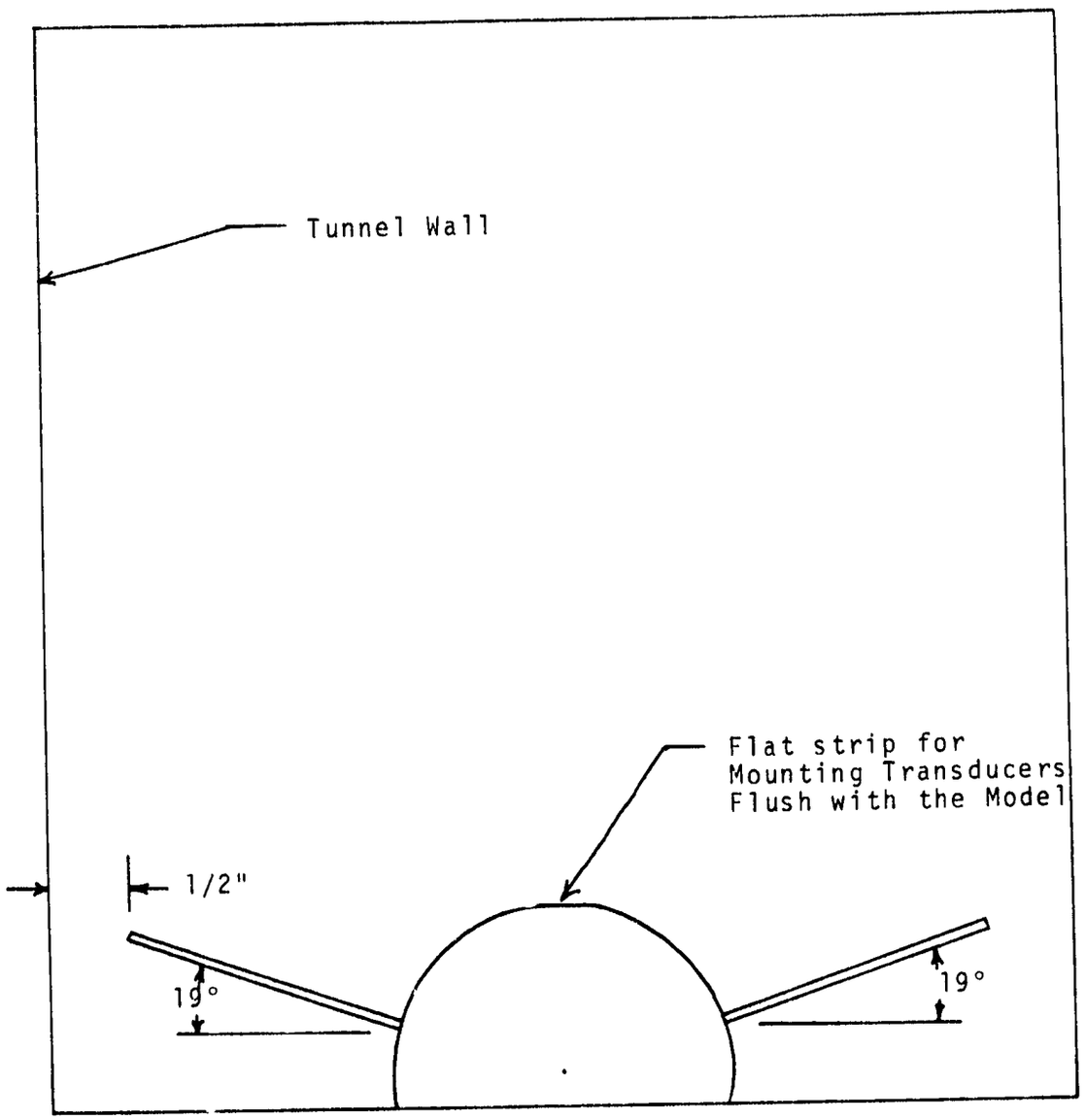

Figure III-2. End View of the Test Model

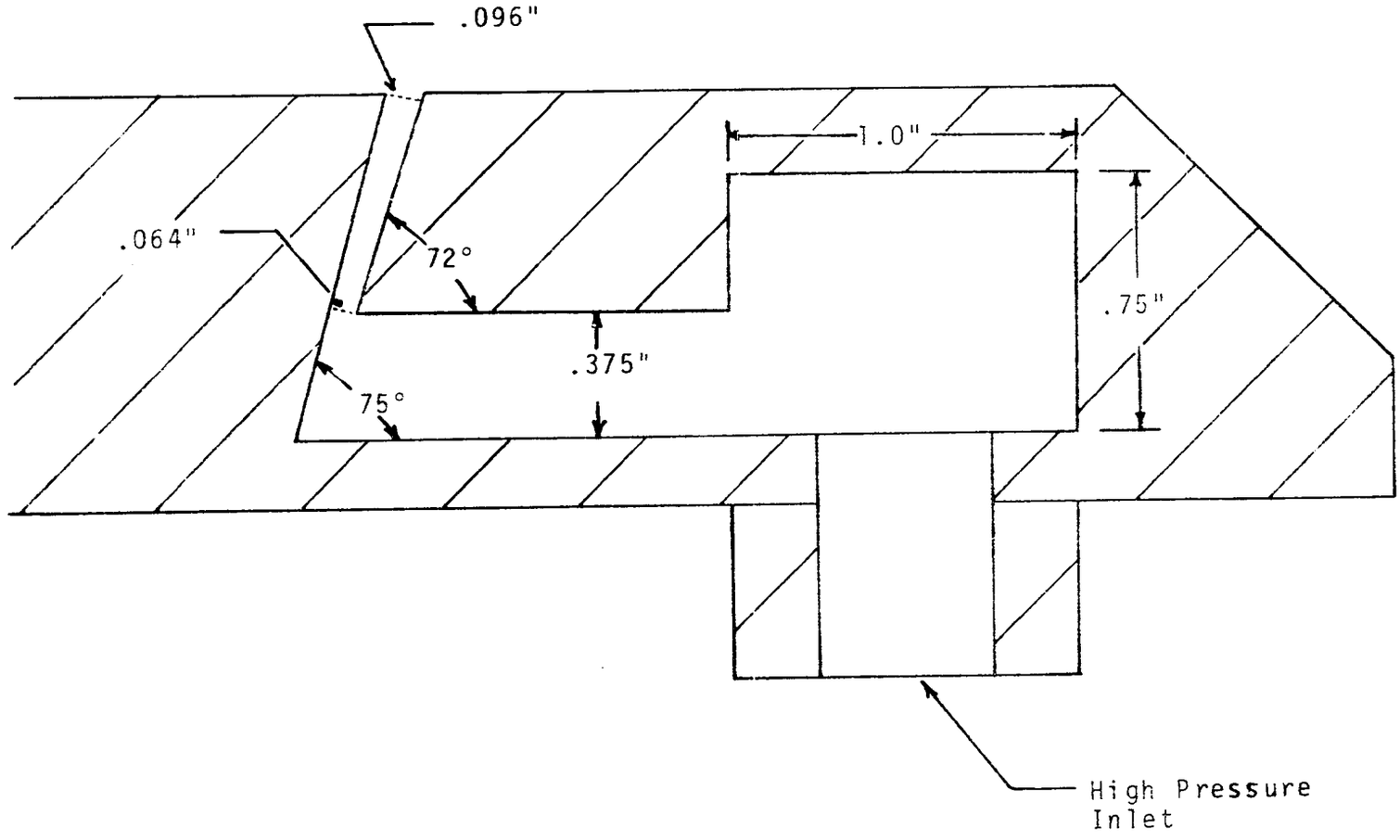

Figure III-3. Cross-Section of the Plume Nozzle Portion of the Test Model

Data Acquisition Systems

Experimental data for this study were obtained from three recording systems. A dynamic system, later referred to as System I, was used to measure and record pressure fluctuating data associated with the separated flow. A static (time-averaged) pressure measuring system, later referred to as System II, provided static pressure profiles for a few sample tests, and a Schlieren system, System III, was used to study the flow geometry.

System I consisted of six Kistler 601-L transducers, six Kistler 553-A charge amplifiers powered by a Kepco D.C. power supply, an Ampex Cp-100 tape recorder, a Tektronix 502-A oscilloscope, and a true RMS Ballantine voltmeter as well as other appropriate electronic equipment.

The transducers used were the piezoelectric type with a resonant frequency of 130,000 HZ and were calibrated with a 160 db, 1 KHZ signal produced by a Photocon acoustic calibrator. Figure III-4 shows the location of each transducer mounted in the model. An electrical schematic of the equipment is shown in Figure III-5. All electrical connections are made with low noise coaxial cable. The equipment used in System I was borrowed from Marshall Space Flight Center.

Signals from the pressure transducer tests were recorded on one inch magnetic tape. Baganoff Associates of St. Louis, Missouri reduced the random signal data to RMS pressure data and power spectral density data.

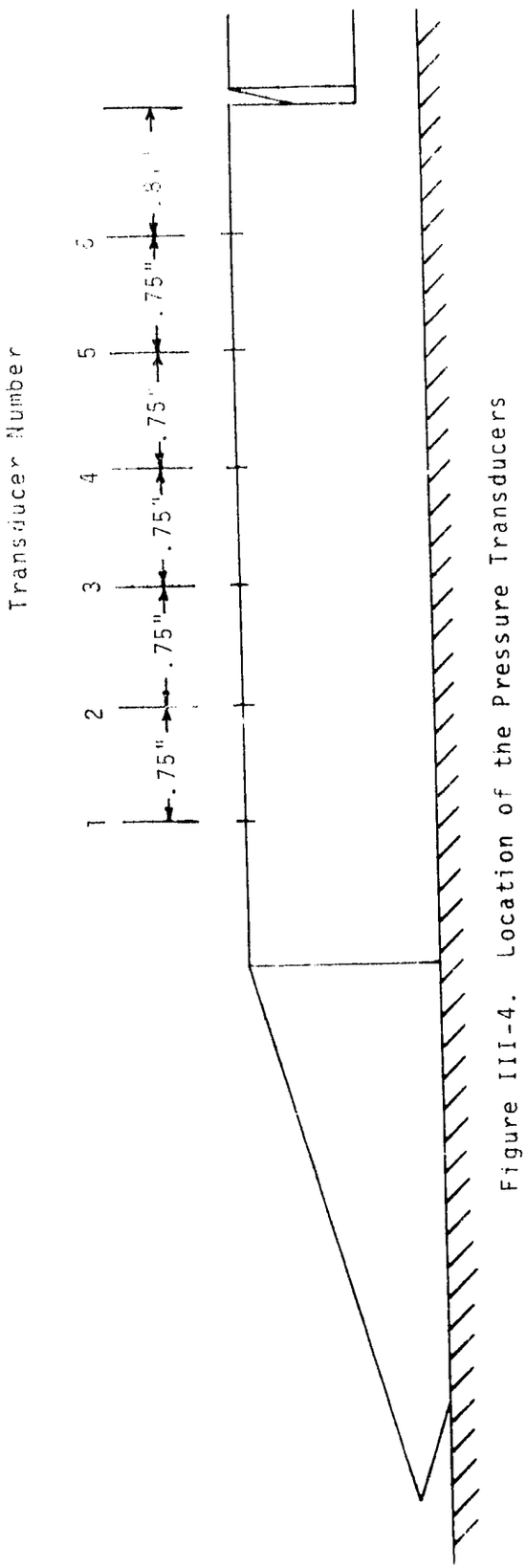

Figure III-4. Location of the Pressure Transducers

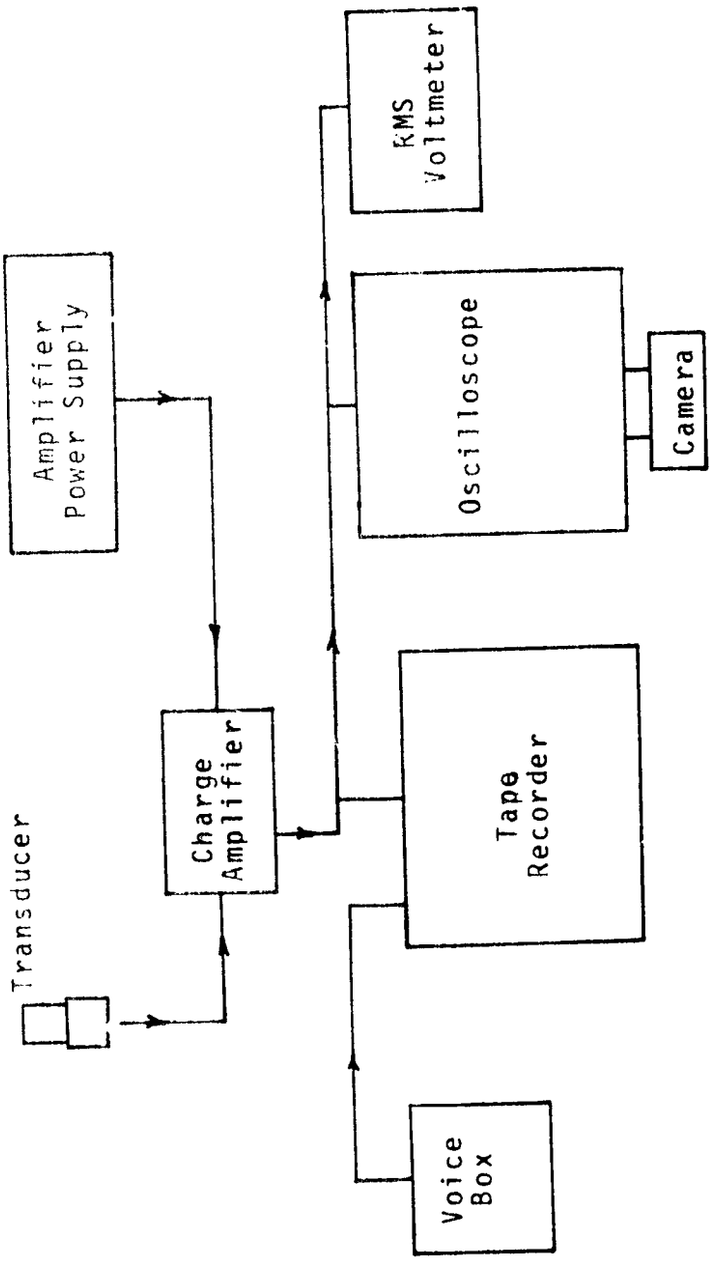

Figure III-5. Schematic Diagram of Electronic Equipment Used in Pressure Fluctuation Tests

System II consisted of six pressure taps (.025 inch diameter orfices) mounted in the model to coincide with the location of the high frequency transducers used in System I, and six USG pressure gages. The mounting holes in the model were designed so that the transducers could be removed and the pressure tap tubes inserted in their place, providing time-averaged and dynamic pressure measurements at identical model locations.

System III consisted of a standard black and white Schlieren system manufactured by Kenny Engineering Corporation. Schlieren photographs were taken by a 35mm Miranda camera. From the Schlieren photographs, separation lengths and shock angles were obtained.

Primary and Secondary Flow Systems

A six inch by six inch supersonic wind tunnel manufactured by Aerolab Supply Company in Hyattsville, Maryland was used to simulate supersonic speeds of the model. The tunnel was designed for continuous Mach number variation in the range of 1.6 to 3.5 by means of a sliding lower nozzle block. It was not possible to obtain the access required for these tests through the walls of the existing test section in the wind tunnel. Therefore, a 13 inch test section extension was designed and constructed for this project. (See Figure III-6). The extension was mated to the original test section as carefully as possible, and no

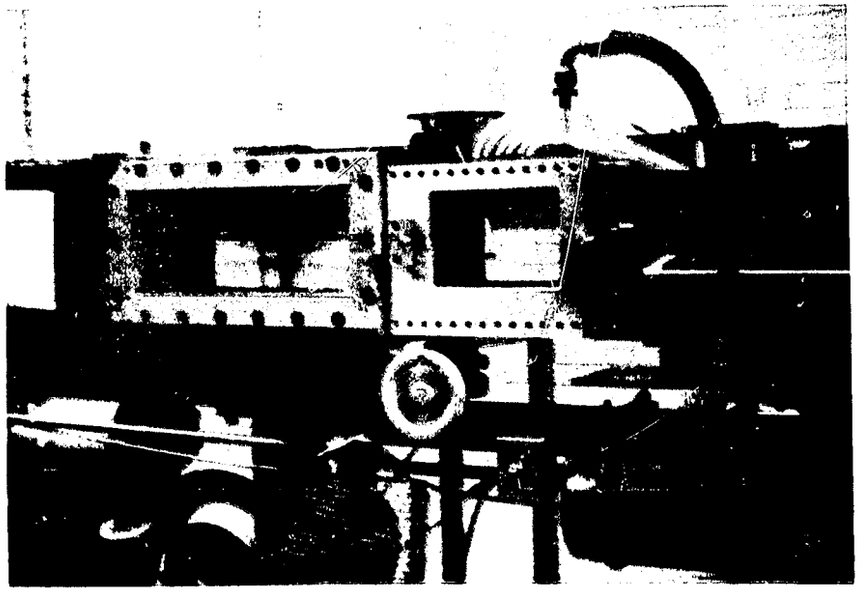

Figure III-6. Supersonic Wind Tunnel Test Section

flow disturbance at the junction was found in Schlieren observation. The windows were made of 8 inch by 6 inch by 1 1/4 inch plate glass. Because the windows were not large enough to observe the entire model, they were located for observation of the plume-separation region. It should be noted that the tunnel calibration was performed by Martin [15] before a new pneumatic control valve system and the extended test section were installed. In a preliminary test a portion of the lower nozzle block failed, and it was necessary to dismantle the tunnel and make repairs. The repairs were very closely supervised, and with several test runs it was determined that the tunnel was repaired with virtually no change in calibration.

The plume flow was created by the secondary flow system which consisted of a high pressure test facility located near the wind tunnel. Air at 2400 psi and near room temperature was brought to the plume control panel in front of the wind tunnel by two 1/2 inch stainless steel tubes. The plume pressure was regulated by a Tescom dome regulator before the air entered a stainless steel settling chamber at which point the plume stagnation pressure was measured on a ten inch Heise gauge. A three foot section of 3/4 inch flexible high pressure hose connected the settling chamber and the model.

Test Procedure

All tests in this investigation were conducted in essentially the same manner. The plume flow was established first and maintained throughout the tunnel run.* Mach numbers were varied from 2.5 to 3.5 in increments of 0.2, and plume pressures were varied from zero psi to 800 psi in increments of 200 psi. Arrangement of the test facilities necessitated separate tests for each type of test; that is, the tests to measure fluctuating pressures, to measure static pressures, and to obtain Schlieren photographs were conducted separately.

---

* It was surprising to the investigators that the plume flow did not block the tunnel and prevent a start, however, good flow could be established with the plume in operation. It is noted that this indicates at least one major behavioral difference in plume flow and that simulated by a solid body.

CHAPTER IV

DISCUSSION OF RESULTS

This section includes a presentation of selected data collected in this investigation. Trends and magnitudes are shown and comparison is made with similar data associated with separation induced by solid body configurations

Flow Geometry Data

Because of the unusual mounting arrangement of the model used in these tests (i.e., a wall mounted cylinder) assurance was sought that the flow in the vicinity of the separation region was not disturbed. That assurance was found from oil flow patterns, Schlieren studies, and surface pressure measurements. In each instance, as will be discussed, there were no significant effects found of the mounting arrangement on the flow over the upper surface of the model

Oil flow studies were conducted before the instrumentation of the model. The patterns obtained did not have sufficient contrast for good quality photographs; however, close observation of the patterns showed that the splitter fins did isolate the main body of the model from the tunnel boundary layer. The patterns also indicated that the plume boundary was contained by the fins for a plume stagnation

pressure up to 800 psi. The general conclusions of this was that the flow in the plume and instrumentation regions was essentially as it would have been had the model and flow been completely axi-symmetric.

Mean static wall pressures were obtained for a Mach number of 2.7 over a range of plume pressures. These profiles are shown in Figure IV-1, in which the five plume pressure conditions are shown in a vertically staggered arrangement to facilitate comparison of the profiles for different plume pressures. The no-plume profile shows constant wall pressure within experimental error and again supports the conclusion that the flow in the instrumentation region was not disturbed by the mounting arrangement.

The Schlieren photographs in Figure IV-2 illustrate typical flows studied in this project. Only the upper surface of the cylindrical section of the model is visible, with the plume and separation in the lower left region of the photographs. The shocks running diagonally across the field (excluding the separation shock) are generated in the nose region of the model. Again there are no indications of flow disturbance due to mounting in the instrumentation region.

The black strip showing in the field of the photographs is a two inch reference length. From this the separation length was measured, taking the intersection of the separation shock and the model surface as the point of separation and defining the separation length to be the distance from

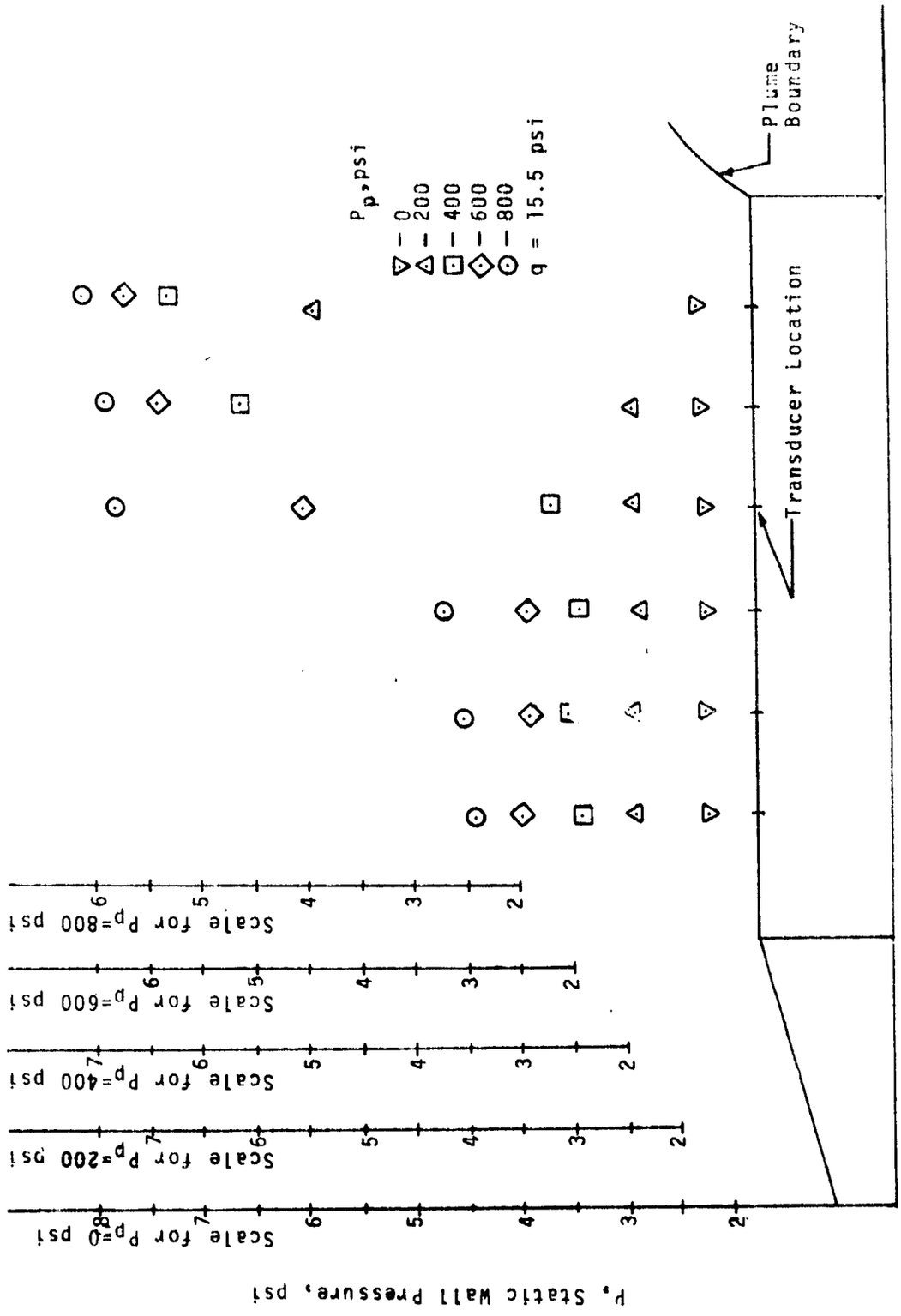

Figure IV-1. Mean Static Wall Pressure Profiles for Various Plume Stagnation Pressures, M=2.7

a. M=2.7, P_p=200 Psi

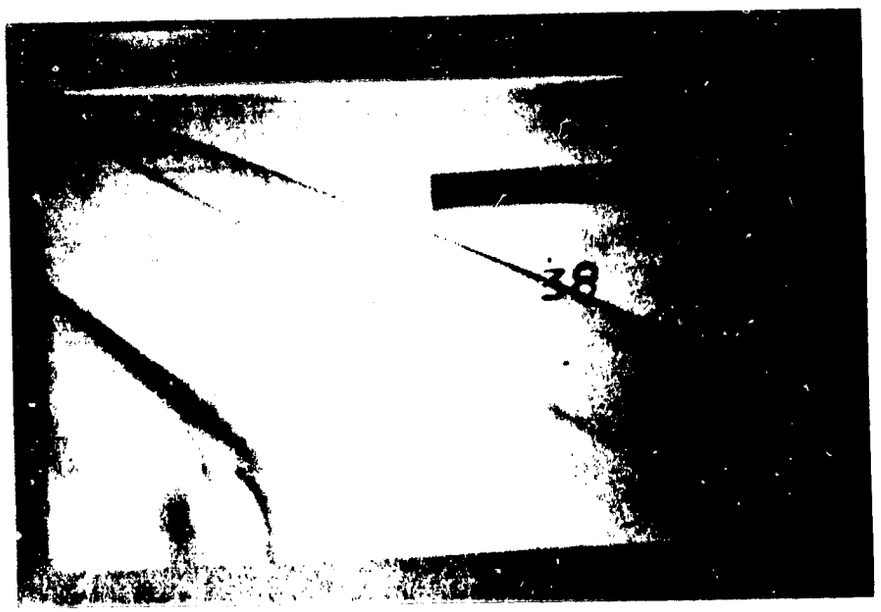

b. M=2.7, P_p=400 Psi

Figure IV-2. Schlieren Photographs of Plume Induced Flow Separation

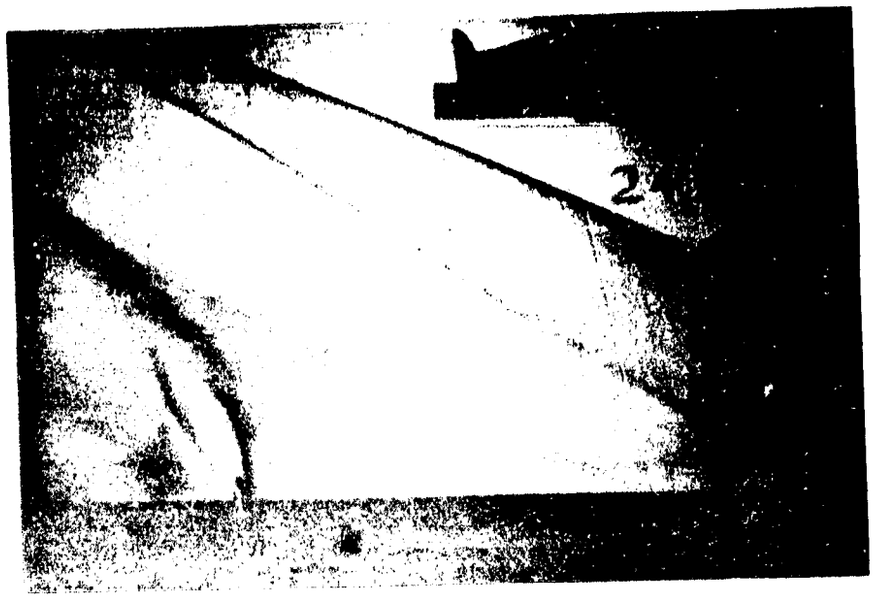

c. M=2.7, P_D=600 Psi

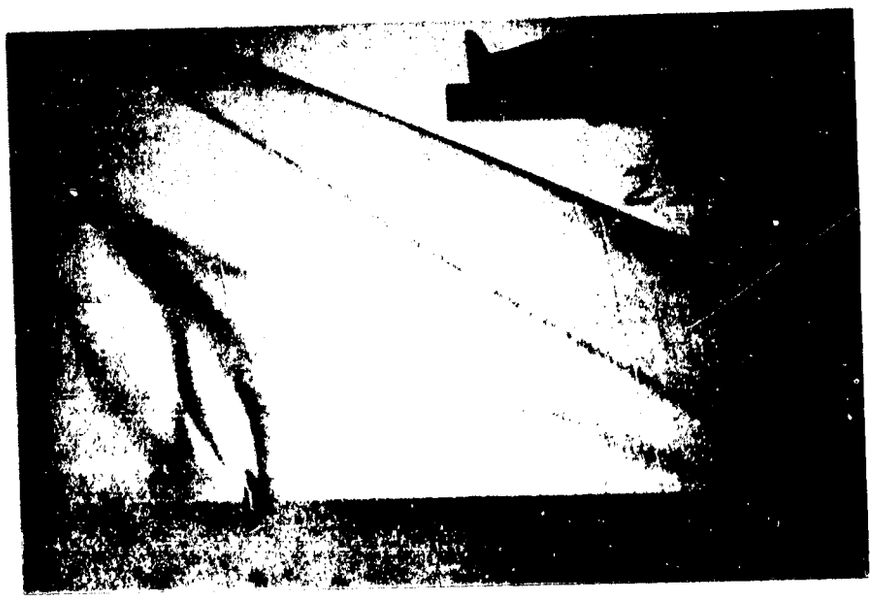

d. M=2.7, P_D=800 Psi

Figure IV-2 (Continued)

that point to the plume origin. Figure IV-3 presents separation length versus normalized plume pressure for each Mach number. Gillette [8], Williams [19], and Mikesell [16] observed a Mach number effect on separation length, however, if there is a Mach effect present in this study it is obscured by data scatter. The data in Figure IV-3 could be approximated by one smooth curve.

Separation shock angle data are shown in Figure IV-4. The angle decreases with increasing Mach number as one would expect. Also, the curves of separation angle versus plume pressure show negative slope which becomes less negative as the Mach number increases.

Pressure Fluctuation Data

The basic nature of the fluctuating pressure signals is shown by oscilloscope samples in Figure IV-5. A one KHZ, 160 db RMS calibration signal is included with each pressure signal for a frequency and magnitude reference. The signals of transducers one and two, which are ahead of the separation front, appear as a normal turbulent signal. In this instance, the separation front is located near transducer three which produces a signal of an obviously different character in that it includes distinct "steps" which suggest that the shock front is passing back and forth across the transducer. Transducers four, five, and six are located in the separation region and produce signals of a character similar to those

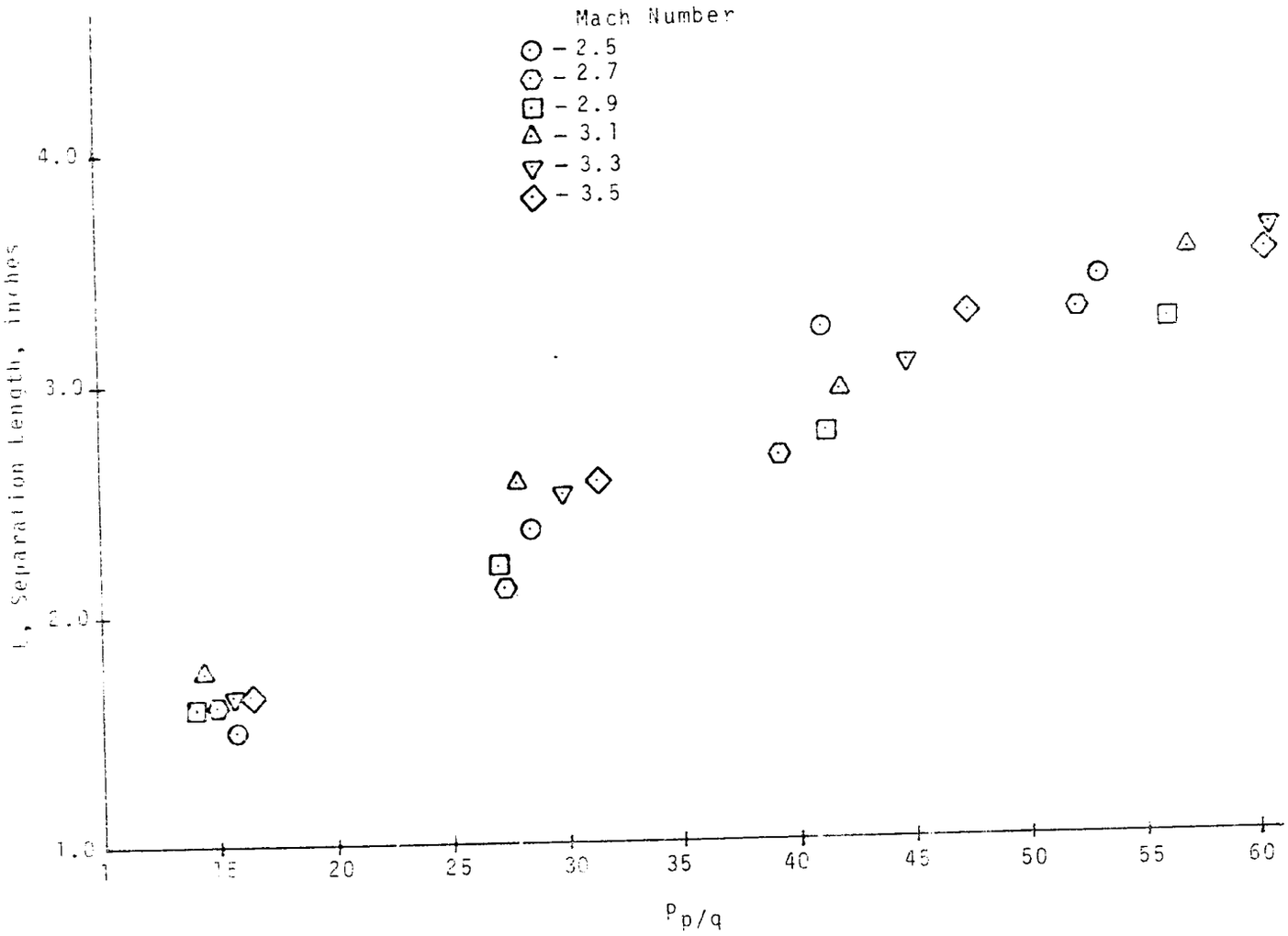

Figure IV-3. Separation Length Versus Normalized Plume Stagnation Pressure for Various Mach Numbers

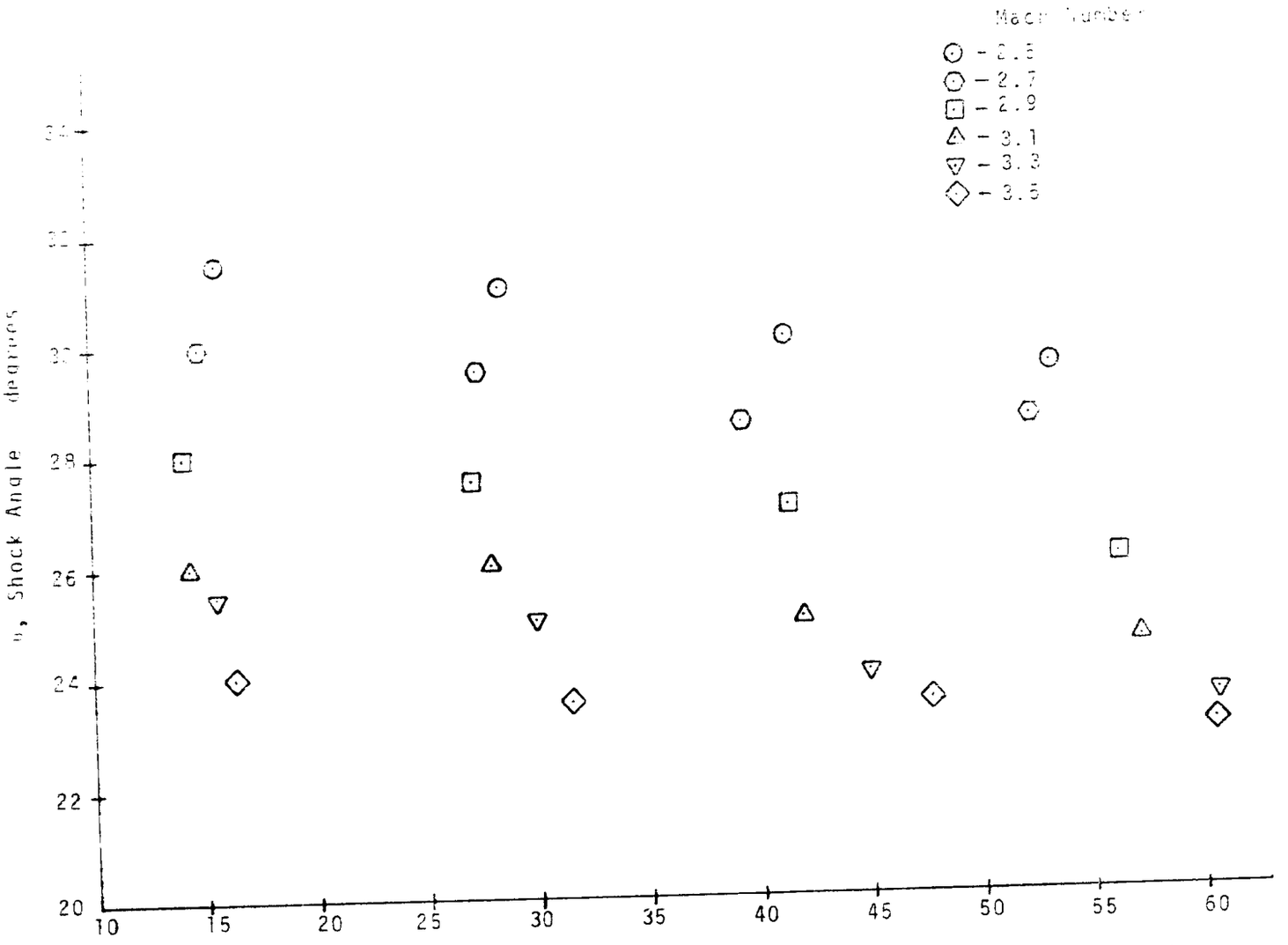

Figure IV-4. Separation Shock Angle Versus Normalized Plume Stagnation Pressure for Various Mach Numbers

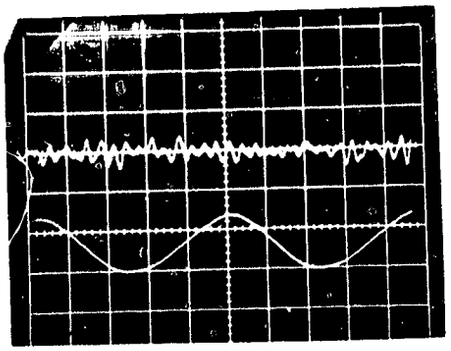

a. Transducer No. 1
(in Front of Shock)

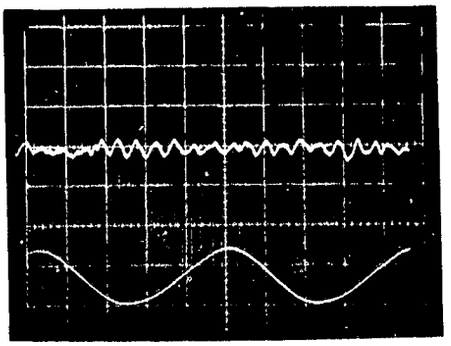

b. Transducer No. 2
(in Front of Shock)

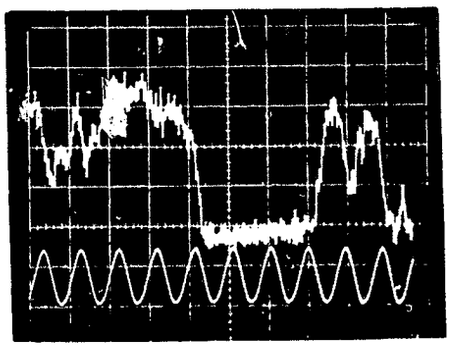

c. Transducer No. 3
(At Shock)

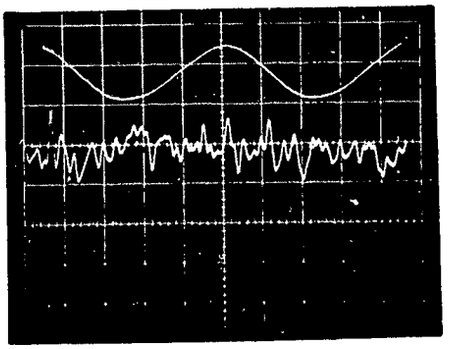

d. Transducer No. 4
(Behind Shock)

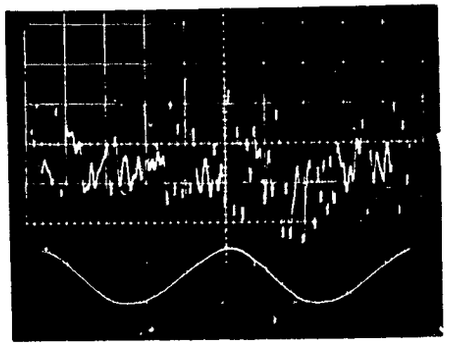

e. Transducer No. 5
(Behind Shock)

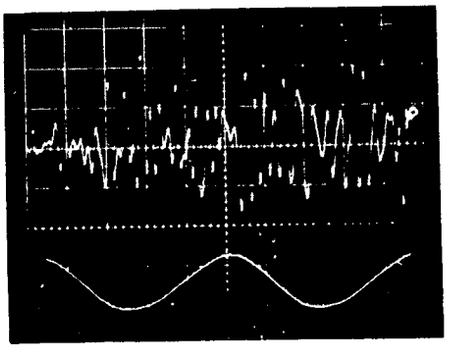

f. Transducer No. 6
(Behind Shock)

M=2.7, P_p=800 Psi

Figure IV-5. Typical Fluctuating Pressure Signals Compared to a 160 db, 1 KHz Sinusoidal Signal

produced ahead of the separation, except that the magnitude is much greater. The signals are very much like those observed by Kistler [10,11] for a turbulent boundary layer separated by a solid step.

Root-mean-squared pressure fluctuation levels are reported for all test conditions. Figure IV-6 shows the general form of the data. There is a sharp peak in RMS pressure level near or at the separation front. The level drops to a minimum for the separated region just behind the separation front and then slowly increases to values which in some cases exceed the peak level at separation. The trend is identical to that reported by Coe [5] except that he did not report the significant rise in the separated region.

Figure IV-7 through IV-12 present the RMS levels obtained in this investigation. The data have been shifted in a horizontal direction so that separation points coincide for different plume pressures at the same Mach number. In several tests the separation point is located between transducers, and tests of this type do not display the peak at separation. This fact along with the data scatter necessitates careful observation to detect trends.

The general form of the power spectral densities is shown in Figure IV-13. The forms are substantially the same as those reported by Coe [5] except for the rise on the high frequency end (in the 12 to 20 KHZ range). Figure IV-14 through IV-19 show numerical examples of normalized power

spectral densities. Unfortunately, no boundary layer length was available and the model diameter was used as the best length scale available. Also, in interpretating the curves one must remember that the shock front was not positioned on a transducer in all tests so that this spectrum is missing from some of the families. Figure IV-17 illustrates an example of this. On the other hand, Figure IV-18 illustrates a case in which the shock spectrum is clearly evident.

There were slight variations in Reynolds number for each Mach number tested because of small variations in test section stagnation pressure. However, nominal values of Reynolds number can be given for each test section Mach number.

Mach Number	Reynolds Number Per Foot
2.5	0.90×10^7
2.7	1.02×10^7
2.9	1.13×10^7
3.1	1.21×10^7
3.3	1.27×10^7
3.5	1.36×10^7

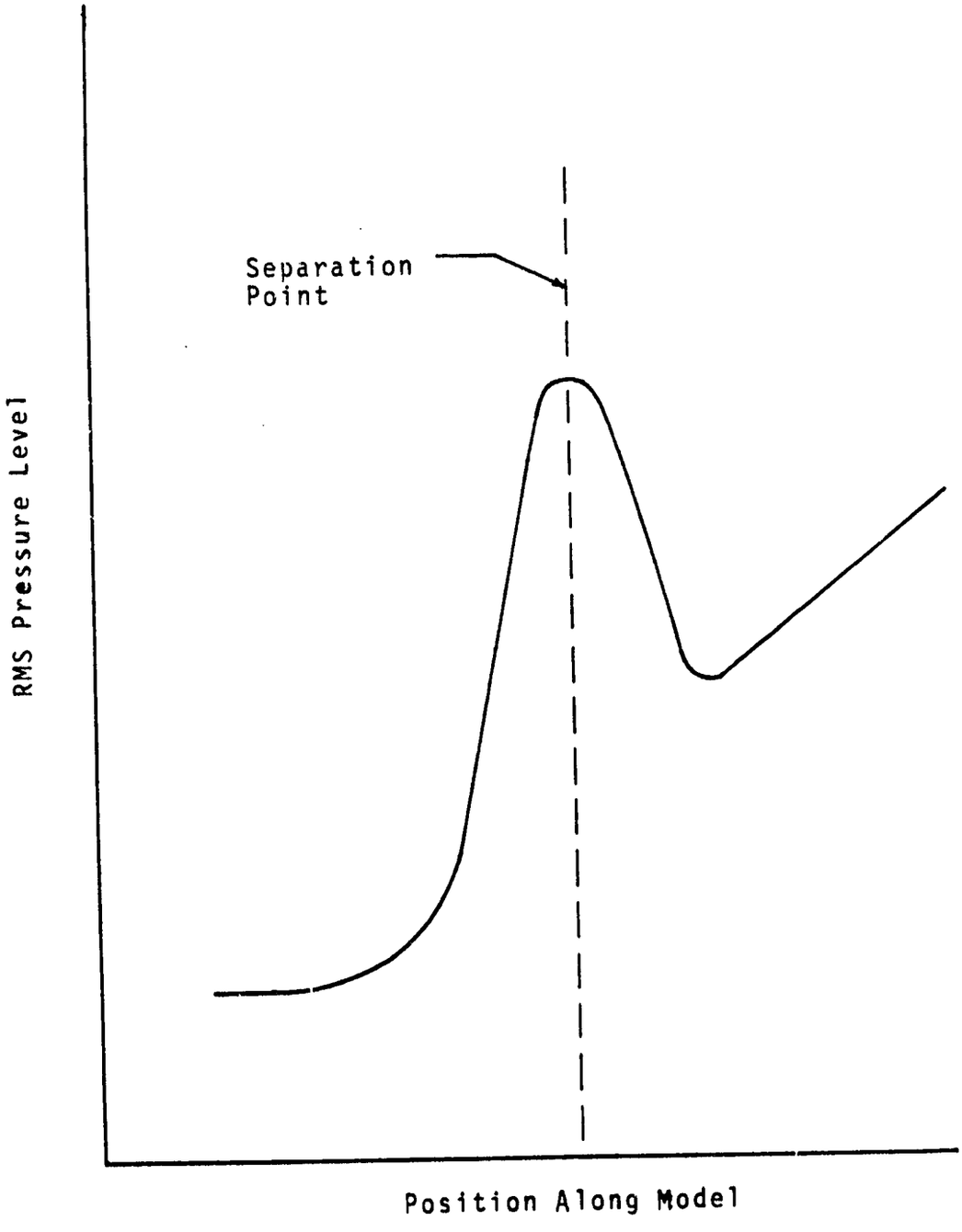

Figure IV-6. General Nature of RMS Pressure Curves

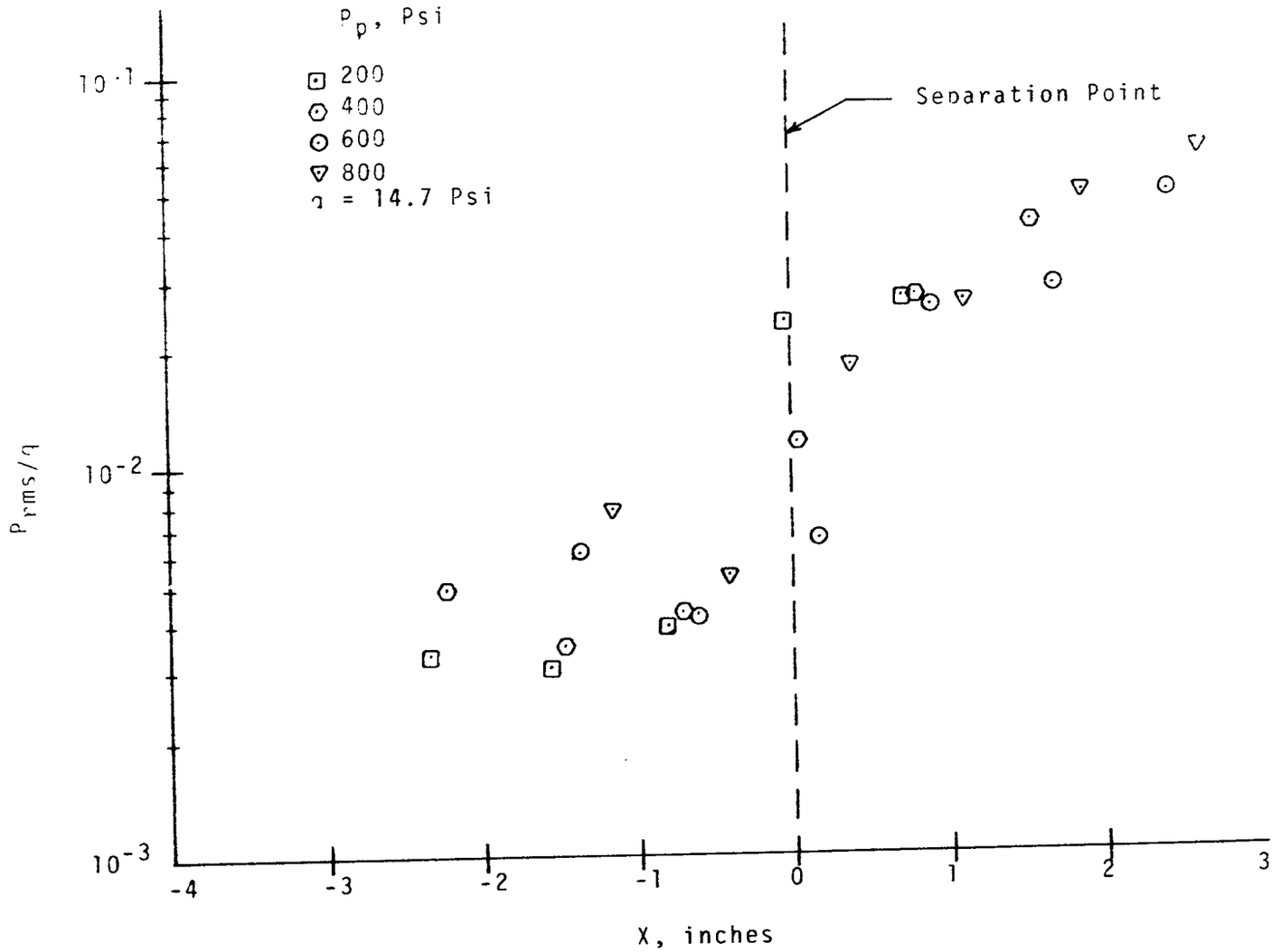

Figure IV-7. RMS Pressure Level Versus Distance from Separation Point for M=2.5

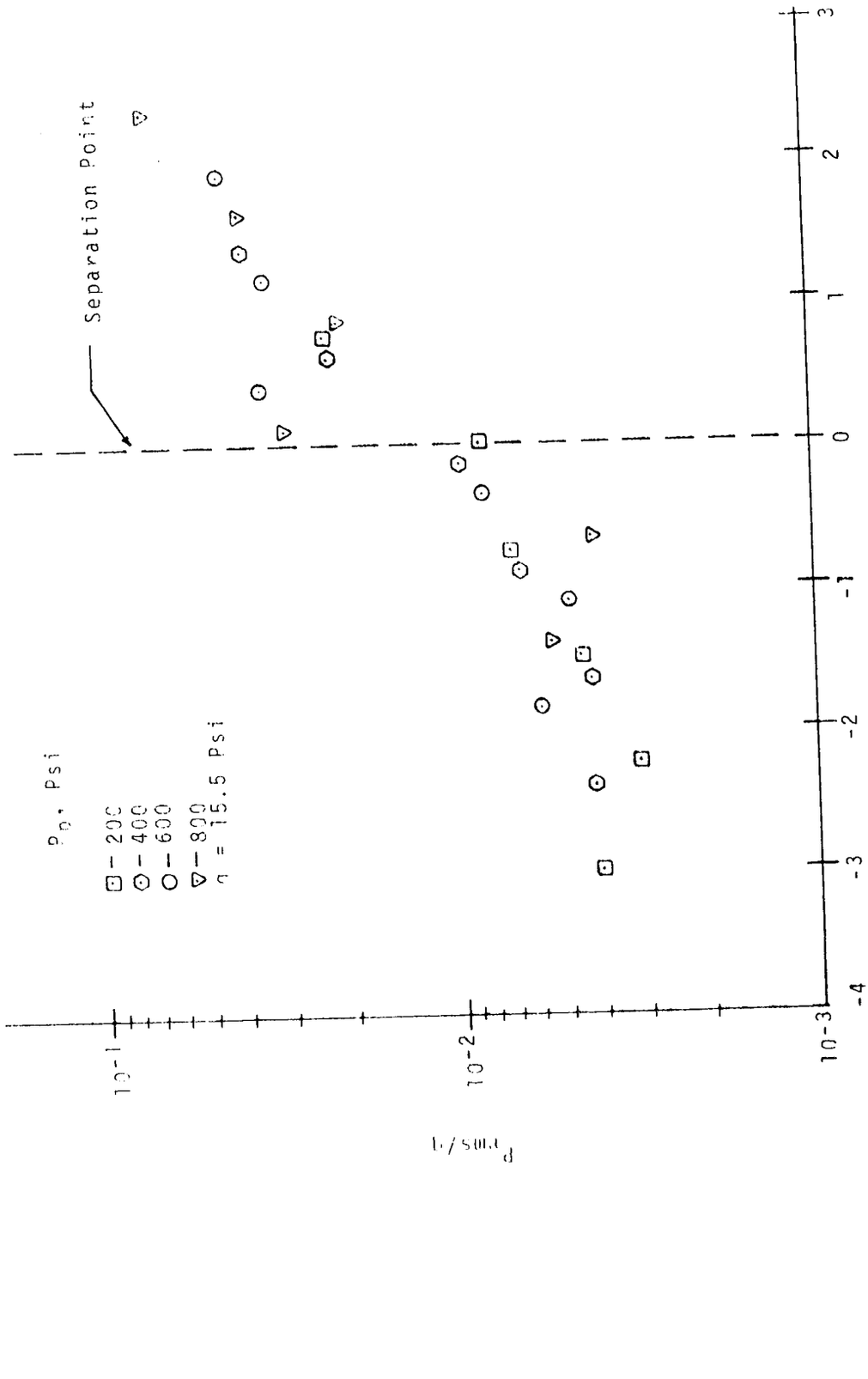

Figure IV-8. RMS Pressure Level Versus Distance from Separation Point for M=2.7

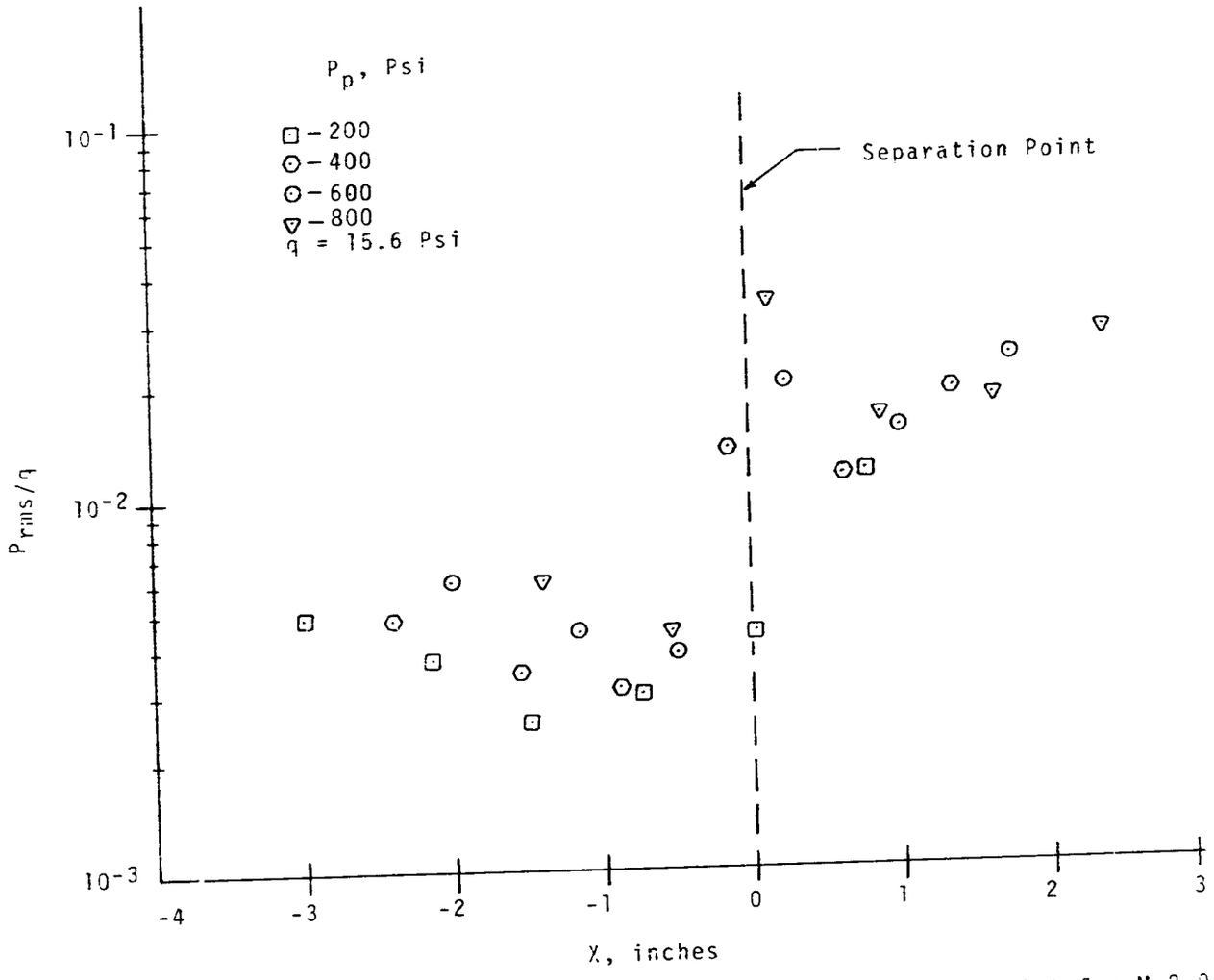

Figure IV-9. RMS Pressure Level Versus Distance from Separation Point for M=2.9

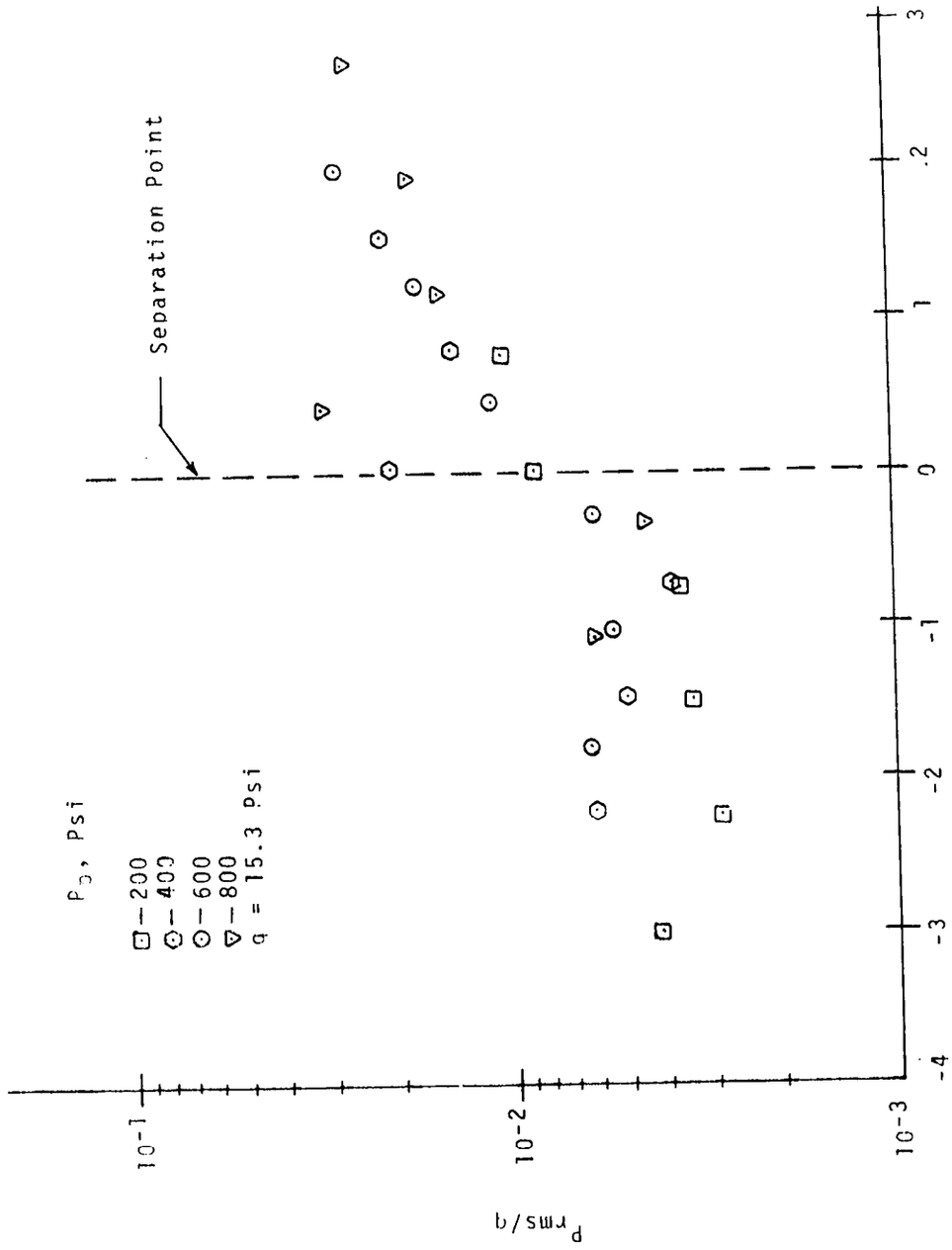

Figure IV-10. RMS Pressue Level Versus Distance from Separation Point for M=3.1

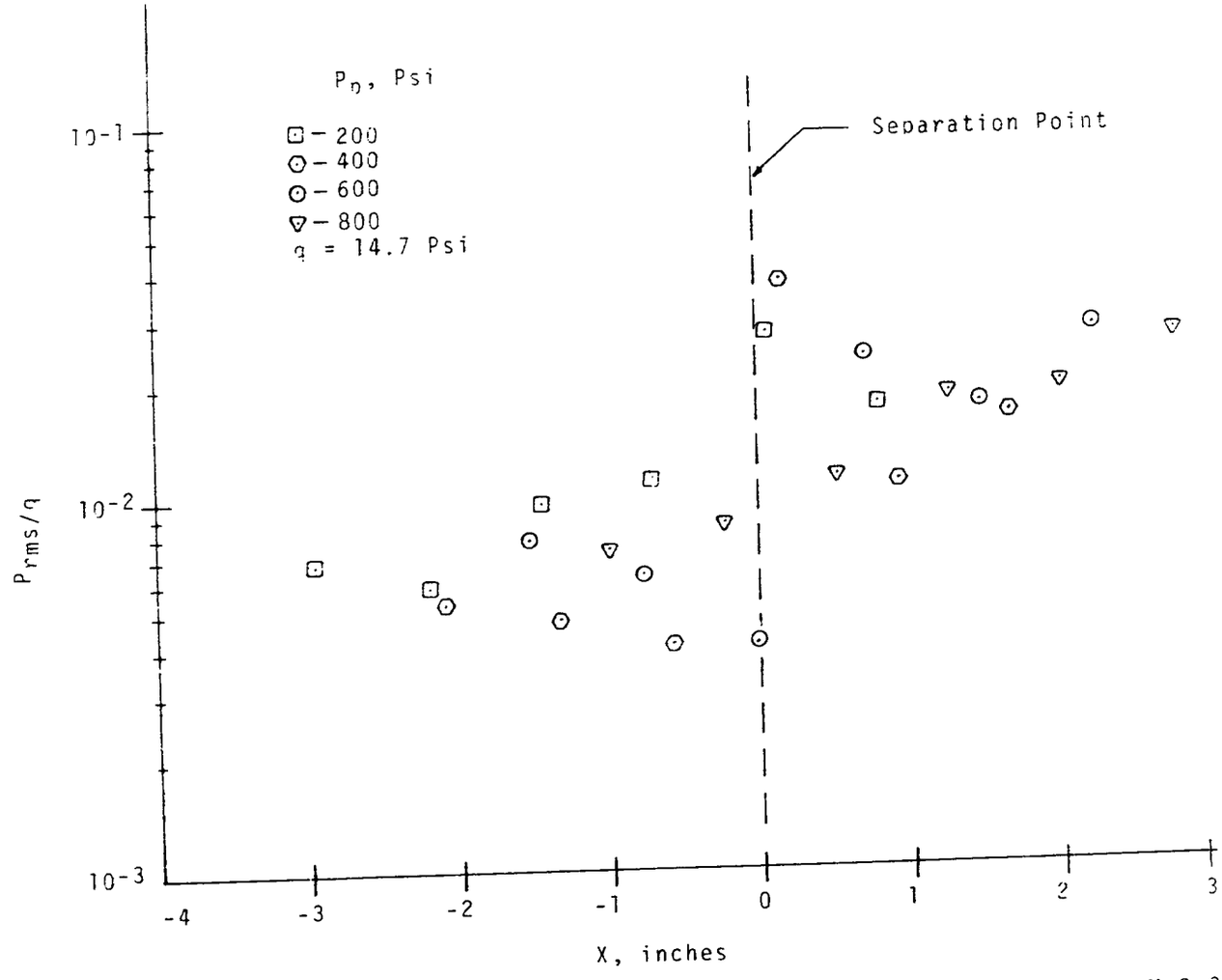

Figure IV-11. RMS Pressure Level Versus Distance from Separation Point for M=3.3

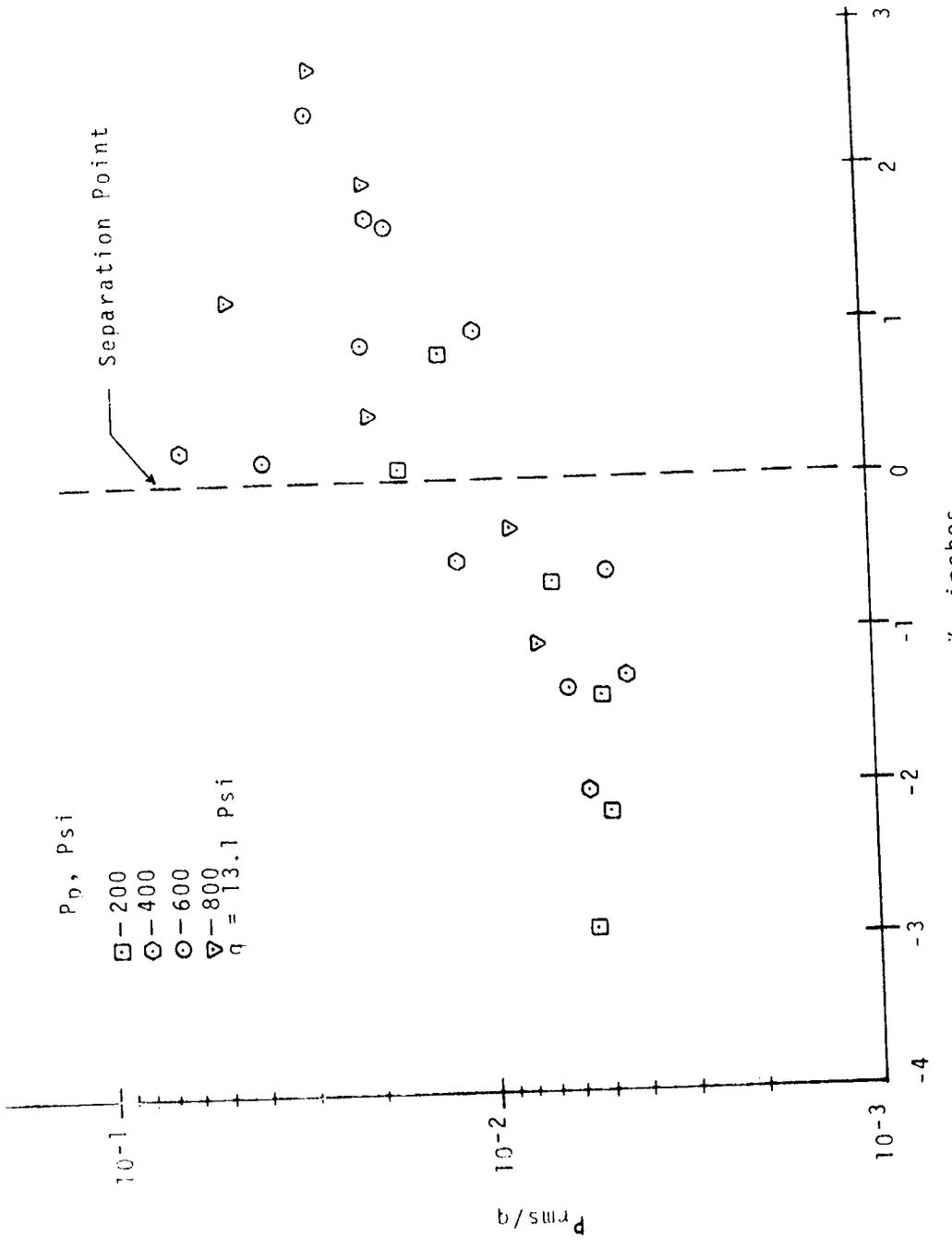

Figure IV-12. RMS Pressure Level Versus Distance from Separation Point for M=3.5

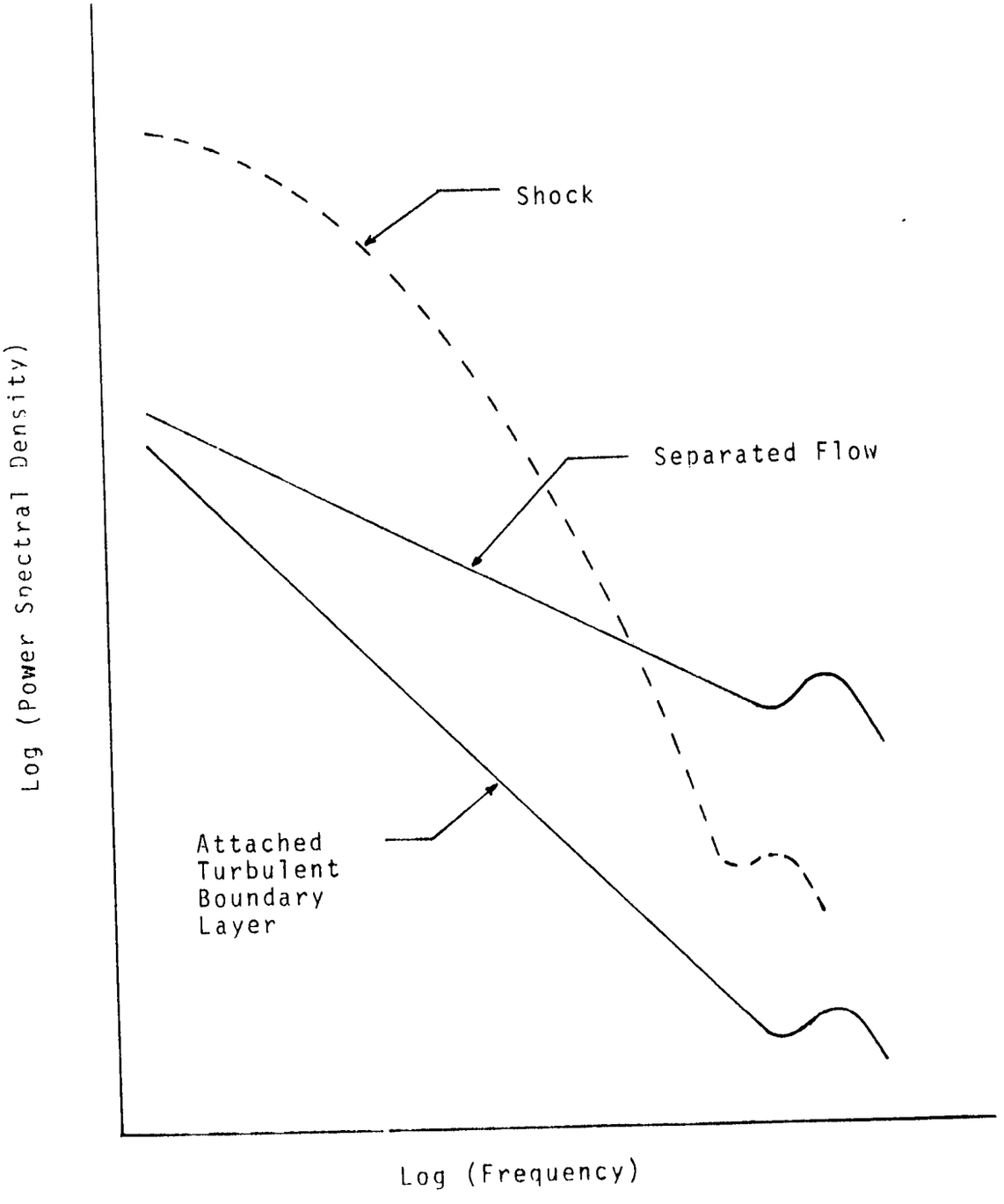

Figure IV-13. General Nature of Power Spectral Density Data

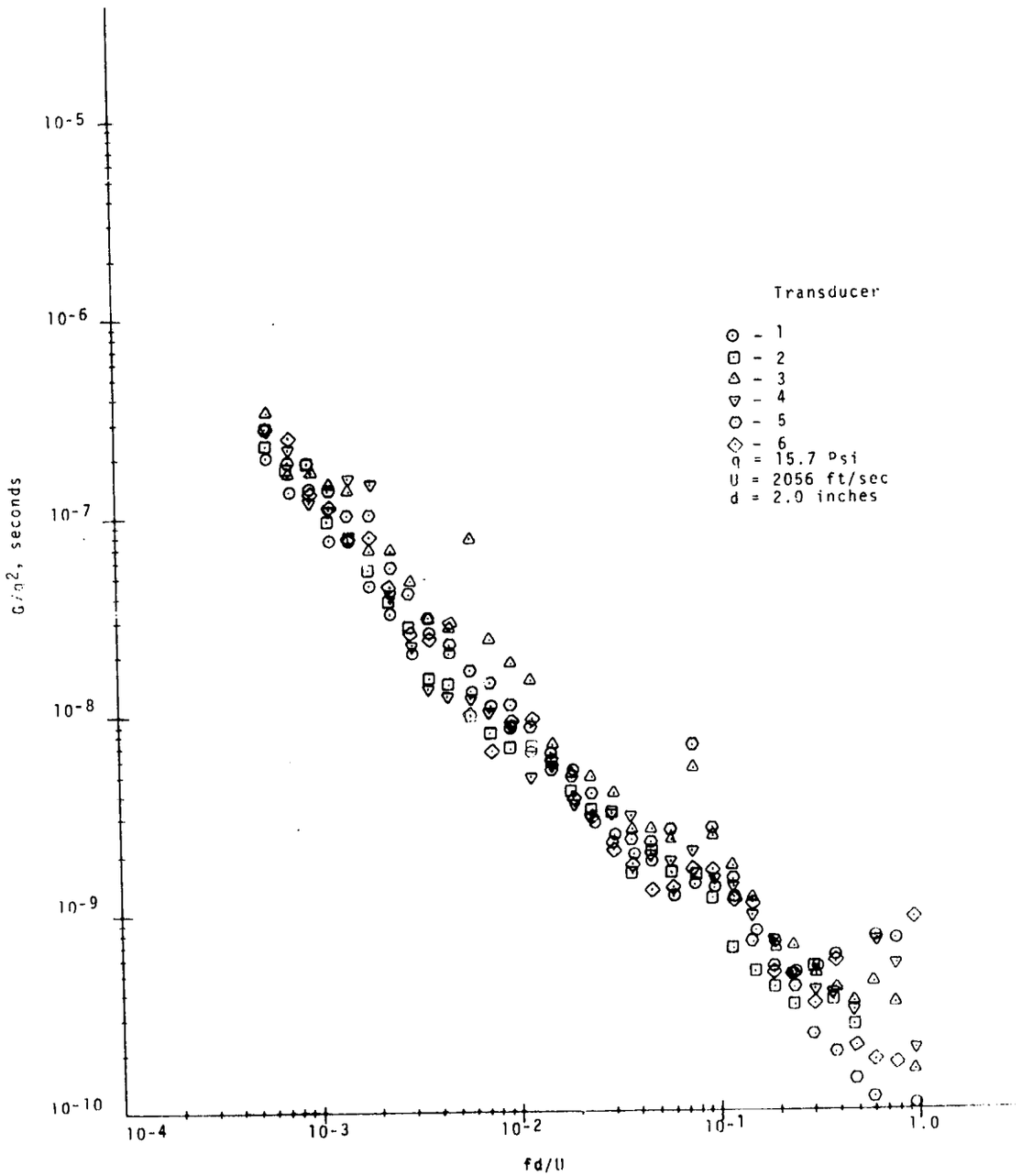

Figure IV-14. Power Spectral Density Data For a Mach Number of 3.1 and a Plume Pressure of 0 Psi

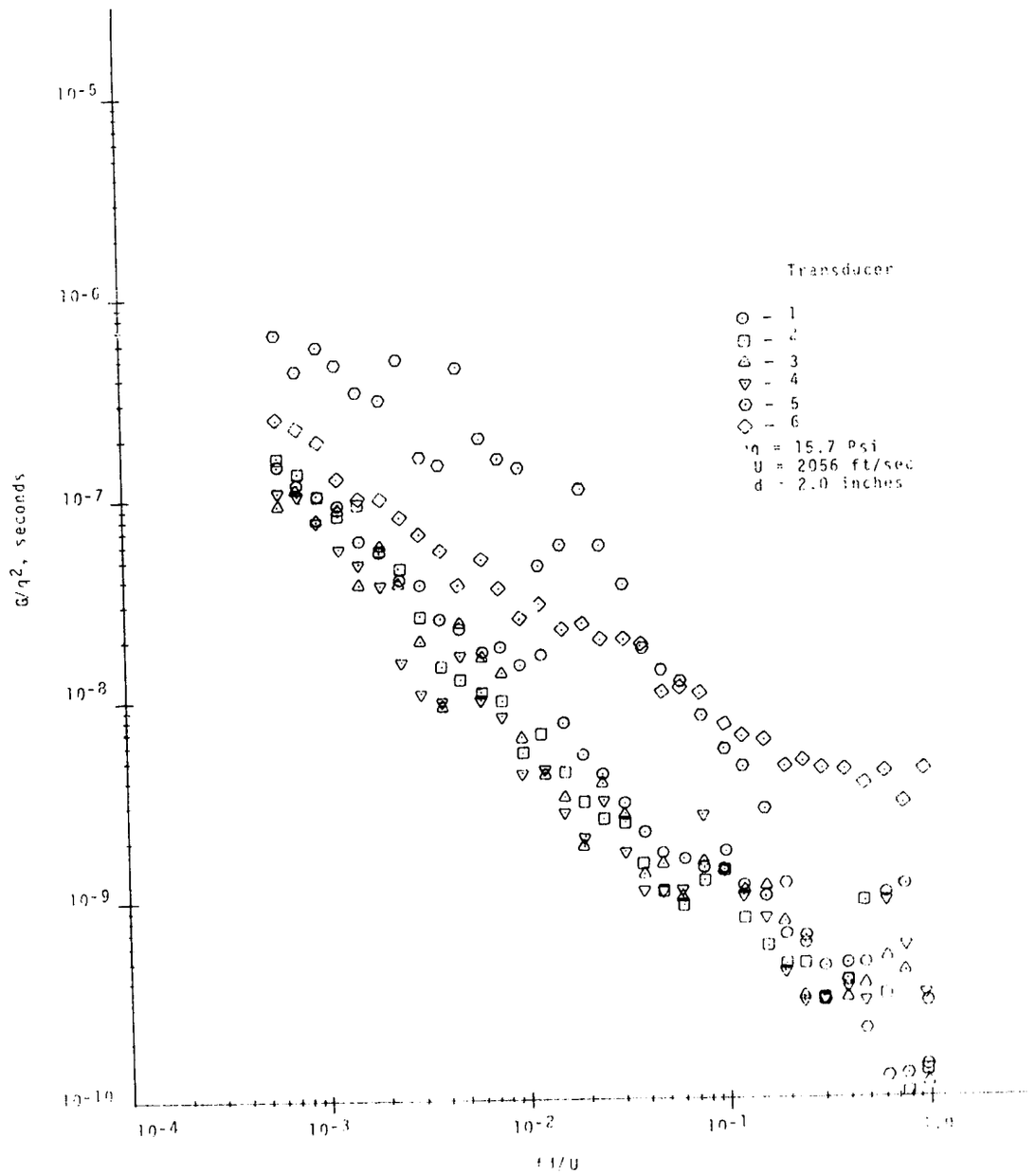

Figure IV-15. Power Spectral Density Data For a Mach Number of 3.1 and a Plane Pressure of [illegible]

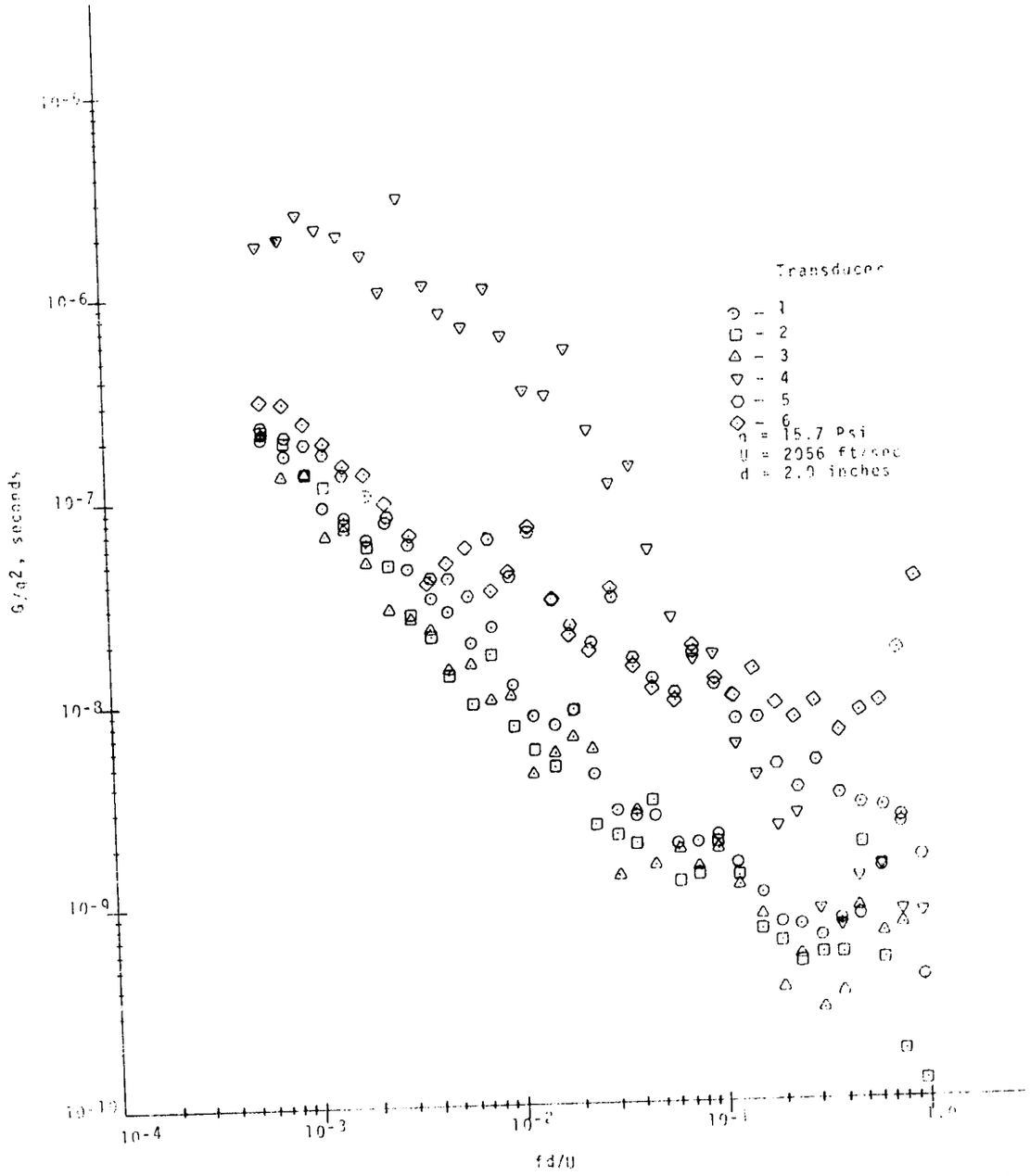

Figure 27-14. Power Spectral Density Data for a Mach Number of 3.1 and a Pitot Pressure of 40 Psi

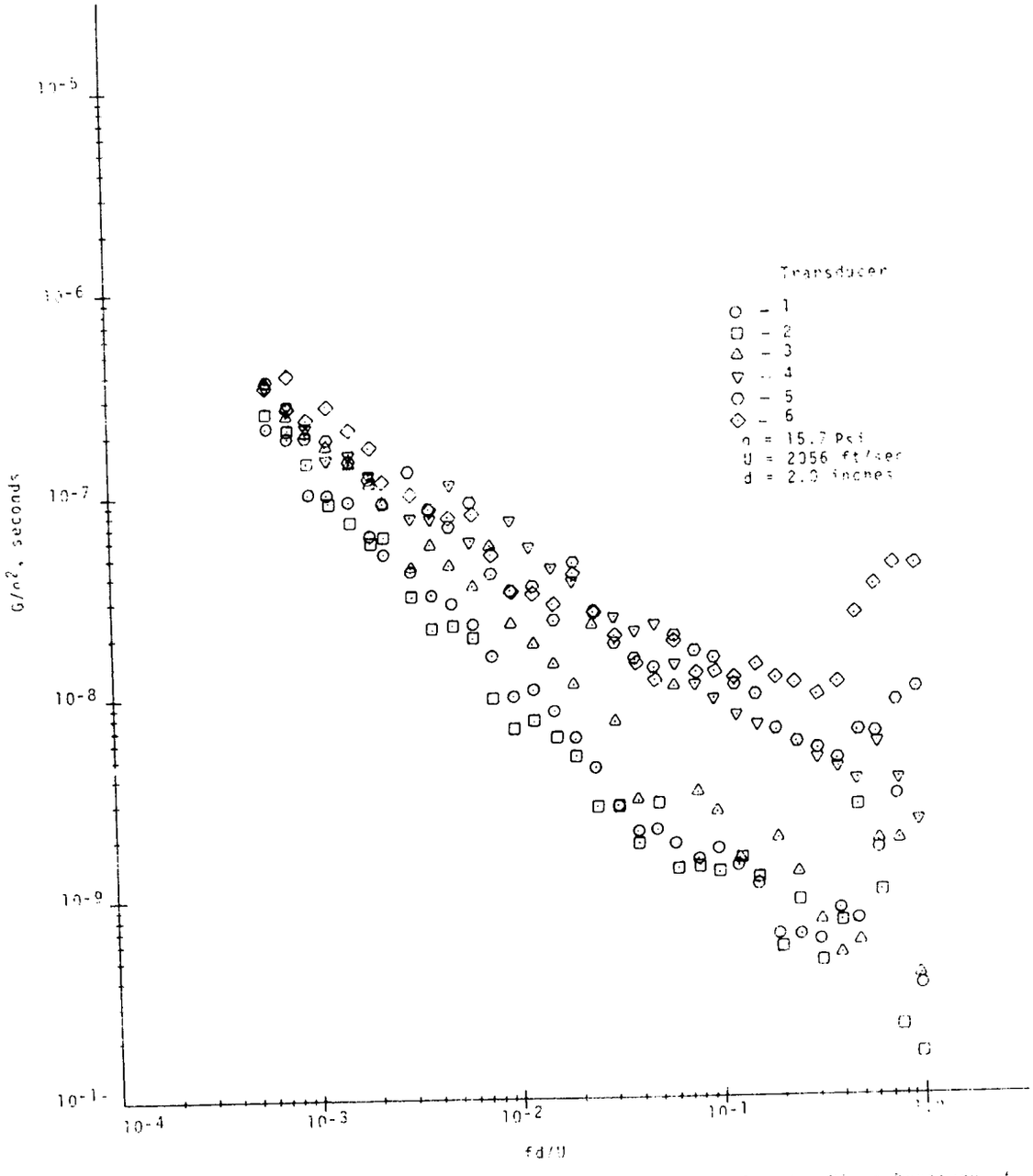

Figure IV-17. Power Spectral Density Data For a Mach Number of 3.1 and a Plenum Pressure of 600 Psi

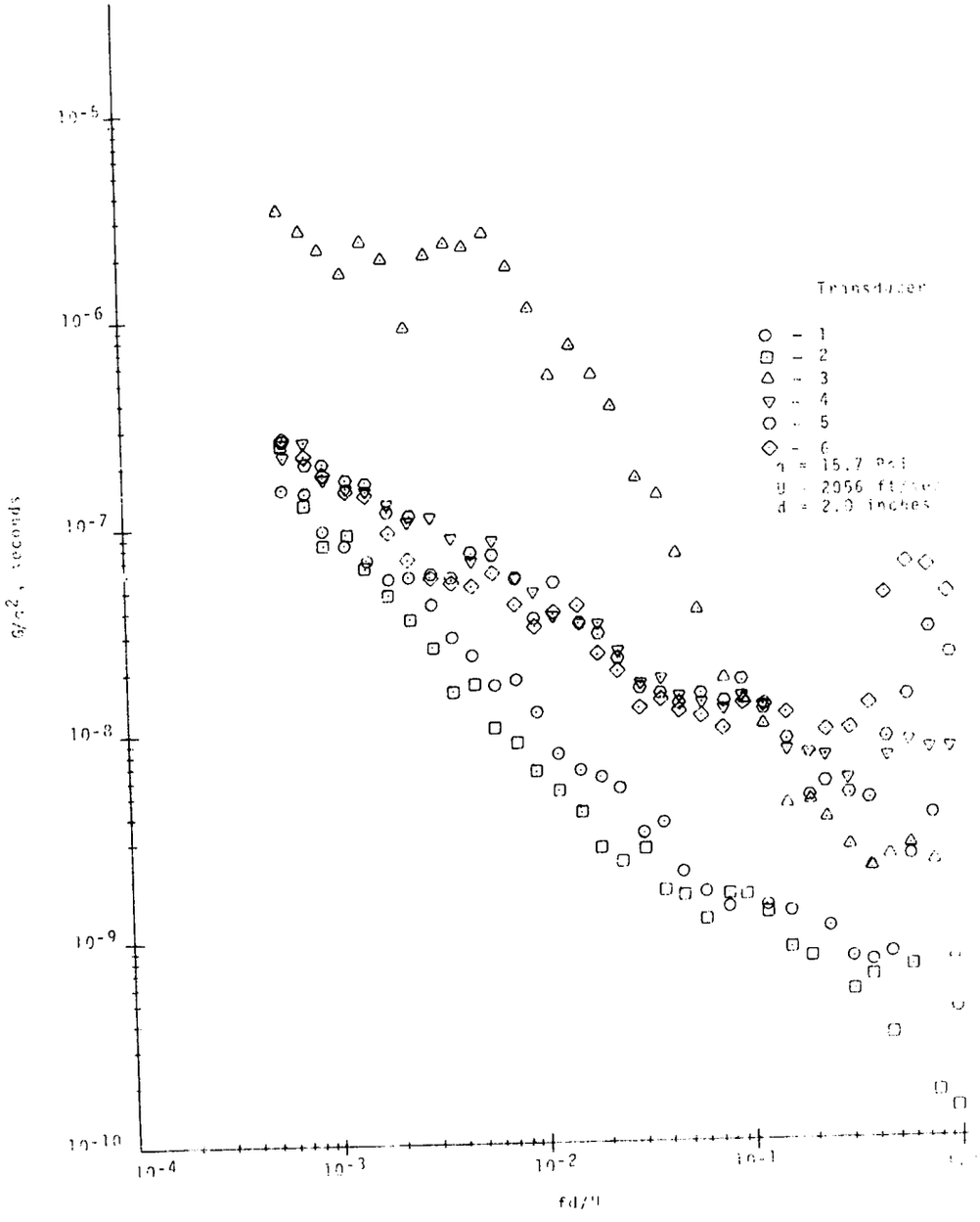

Figure IV-12. Power Spectral Density Data For a Mach Number of 3.1 and a Plate Pressure of 800 Psi

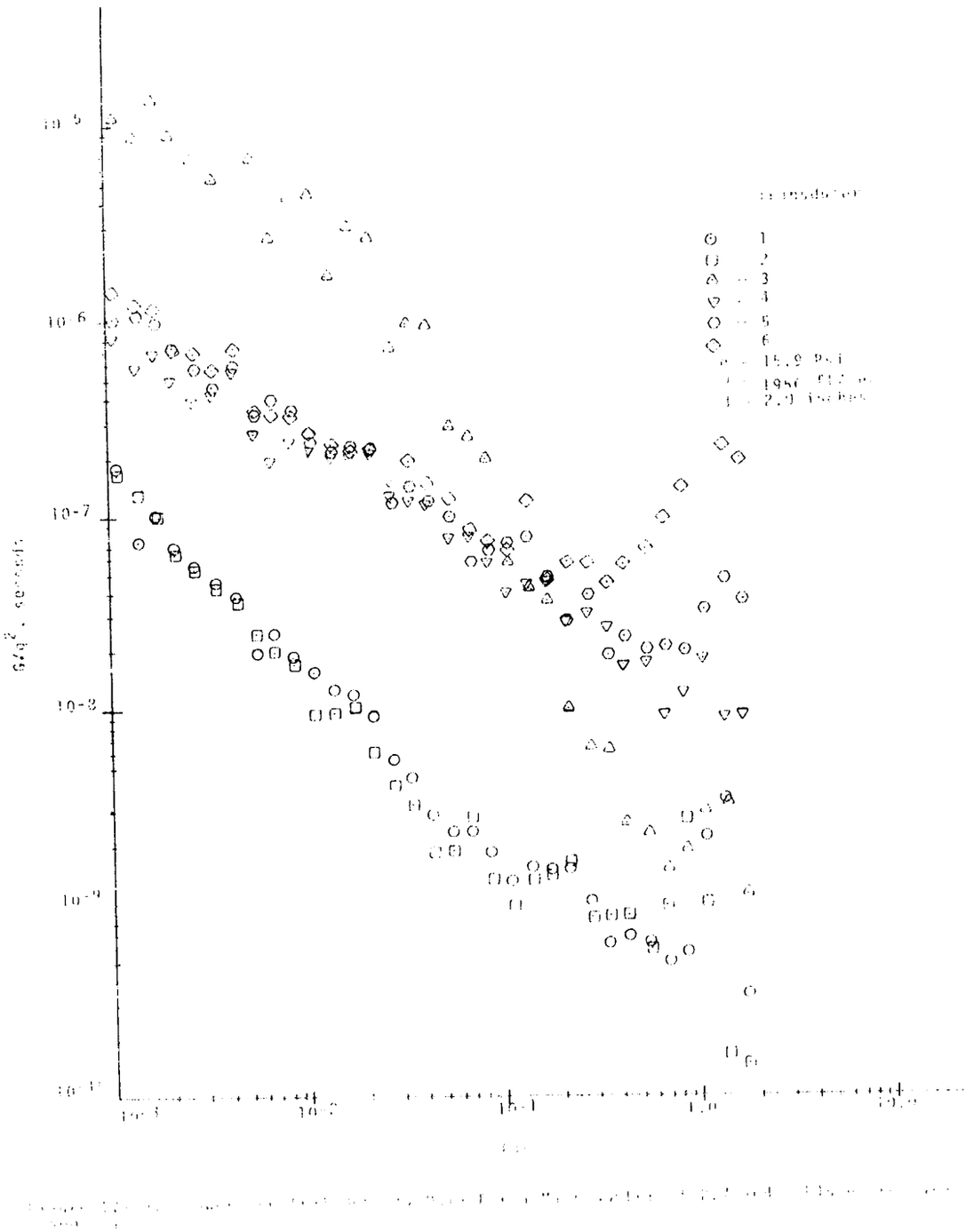

CONCLUSIONS

The RMS pressure levels and power spectral density trends compare in most respects with solid body induced separation data reported by Kistler [10,11] and Coe [5]. However, in this study, the RMS pressure levels in the separated region show a definite increase (after an initial decrease) with distance from the separation point, where as Coe [5] indicates either a constant or slighty decreasing RMS level in the separated region on a solid body. Also, there is a noticeable rise in many of the power spectral density curves for the high frequency range between 12 KHZ and 20 KHZ which is not observed in data associated with solid bodies. The effect is not present in all spectra obtained in this investigation and seems to be most pronounced on spectra for points near, but not on, the separation front.

The pressure fluctuation levels reported by Jones [9] from measurements on a Saturn V flight were not simulated in these tests. A reasonable explanation is that a prototype rocket engine is known to pulse, and no attempt was made to simulate this. Therefore, it is possible that plume unsteadiness can contribute in a major way to the fluctuation in the vicinity of separation.

All testing performed in this investigation indicates that the flow field over the instrumented portion of the wall mounted model was not disturbed by the mounting arrangement. That is, it is possible to simulate body-of-revolution flow by mounting the axis of the body on the tunnel wall boundary layer displacement thickness. Also, it was possible to start the tunnel with the plume in operation even though a much smaller solid body would have blocked the flow.

LIST OF REFERENCES

1. Ames Research Staff: Equations, Tables, and Charts for Compressible Flow. NACA Report 1135, 1953.

2. Blake, W. K.: Turbulent Boundary-Layer Wall-Pressure Fluctuations on Smooth and Rough Walls. J. Fluid Mech., vol. 44, 1970, pp. 637-660.

3. Bogdonoff, S. M.; and Kepler, C. E.: Separation of a Supersonic Turbulent Boundary Layer. J. Aerospace Sci., vol. 22, 1955, pp. 414-424.

4. Chapman, D. R.; Kuehn, D. M.; and Larson, H. K.: Investigation of Separated Flows in Supersonic and Subsonic Streams with Emphasis on the Effect of Transition. NACA Report 1356, 1958.

5. Coe, C. F.: Surface-Pressure Fluctuations Associated with Aerodynamic Noise. Basic Aerodynamic Noise Research Conference, NASA SP-207, 1969.

6. Doughty, J. O.: Some Remarks on Problems Associated with Plume Induced Separation. NASA-ASEE Summer Faculty Fellowship Program, 1970, pp. 219-232.

7. Gadd, G. E.; Holder, D. W.; and Regan, J. D.: An Experimental Investigation of the Interaction Between Shock Waves and Boundary Layers. Proc. Roy. Soc. A-226, 1954, pp. 227-253.

8. Gillette, W. G.: Separation Measurements of Supersonic Turbulent Boundary Layers over Compression Corners. AD 644194, July 1966.

9. Jones, J. H.: Acoustic Environmental Characteristics of the Space Shuttle. Proceedings Space Shuttle Technology Conference, July 1970.

10. Kistler, A. L.: Surface Pressure Fluctuations Produced by Attached and Separated Supersonic Boundary Layers. AGARD Report 458, April 1963.

11. Kistler, A. L.: Fluctuating Wall Pressure Under a Separated Supersonic Flow. J. ASA, vol. 36, March 1964.

12. Kuehn, D. M.: Turbulent Boundary Layer Separation Induced by Flares on Cylinders at Zero Angle of Attack. NACA TR R-117, 1961

13. Love, E. S.: Pressure Rise Associated with Shock Induced Boundary Layer Separation. NACA TN 3601, December 1955.

14. McGhee, R. J.: Jet-Plume-Induced Flow Separations on Axisymmetric Bodies at Mach Numbers of 3.00, 4.50 and 6.00. NASA TN D-3698, November 1966.

15. Martin, T. F.: Calibration of the University of Alabama 6-inch by 6-inch Supersonic Wind Tunnel. M. S. Thesis, University of Alabama, 1971.

16. Mikesell, R. D.: Length Scale of Separated Turbulent Boundary Layers in Compression Corners. AIAA Journal, vol. 4, no. 8, August 1966.

17. Schlichting, H.: Boundary Layer Theory. Sixth Ed., McGraw-Hill Book Co., Inc., 1968.

18. Strike, W. T., Jr.: Jet Plume Simulation at Mach Number 10. AEDC-TR-118, 1970.

19. Williams, J. C.: On the Upstream Length of Turbulent Boundary Layer Separation. AIAA Journal, vol.3, no. 12, 1965.

20. Zukoski, E. E.: Turbulent Boundary Layer Separation in Front of a Forward-Facing Step. AIAA Journal, vol. 5, no. 10, 1967.